Advanced topics in spectral methods for fluid mechanics

Franco Auteri

Dipartimento di Scienze e Tecnologie Aerospaziali
Politecnico di Milano

Applied CFD, a. a. 2014/15.

Outline

Why spectral methods?

- Very accurate (for instance: stability studies),
- Easy to program
- Strong mathematical foundation (C. Bernardi, Y. Maday, ...)

Recent research trends in spectral methods

- Extend geometrical flexibility of spectral methods,
  - non-Cartesian coordinate systems
  - immersed boundary
- Apply spectral methods to exterior problems, e.g.
  - semi-infinite domains (Laguerre, mapped polynomials, rational Chebyshev,...)
  - infinite domains (Hermite,...)
- Remove periodicity while maintaining quasi-optimal computational complexity, e.g.
  - fast Legendre transform (Iserles, 2011)
- Exotic ODEs or PDEs, e.g.
  - Cahn–Hilliard equation
  - ...

In this talk

I'll present some recent advances in spectral methods for fluid mechanics concerning

- non-Cartesian coordinates;
- semi-infinite regions;
- non-periodic boxes.

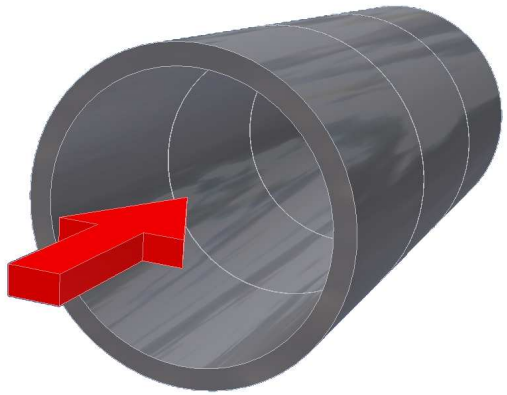

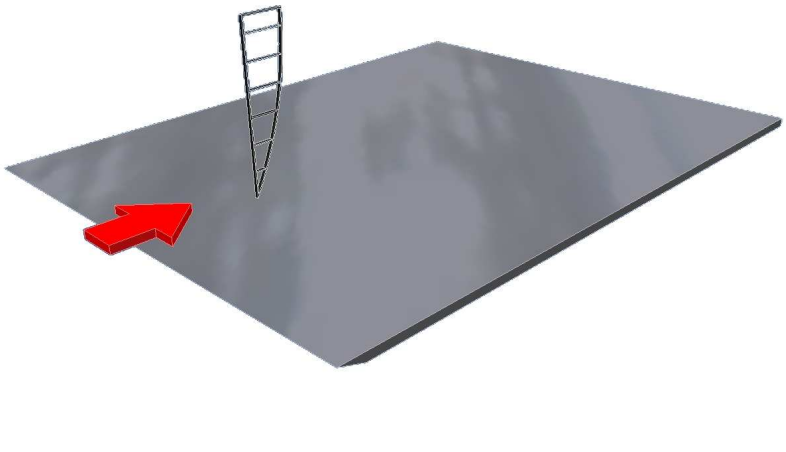

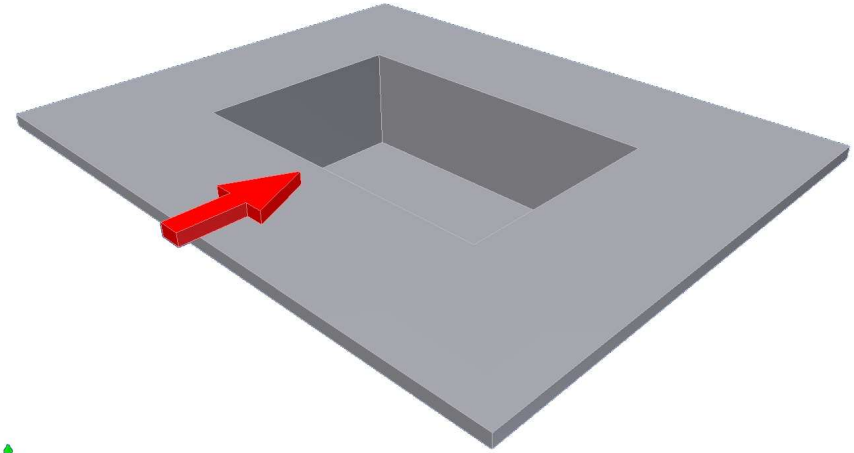

Outline

Accurate and efficient spectral methods in cylinders and spheres

(collaboration with M. Biava, A. Lunghi and L. Quartapelle)

Cylindrical coordinates

- Several problems are usefully set in cylindrical coordinates, for instance: drag reduction experiment (Auteri, Baron, Belan, Campanardi, Quadrio, Phys. Fluids 2010)

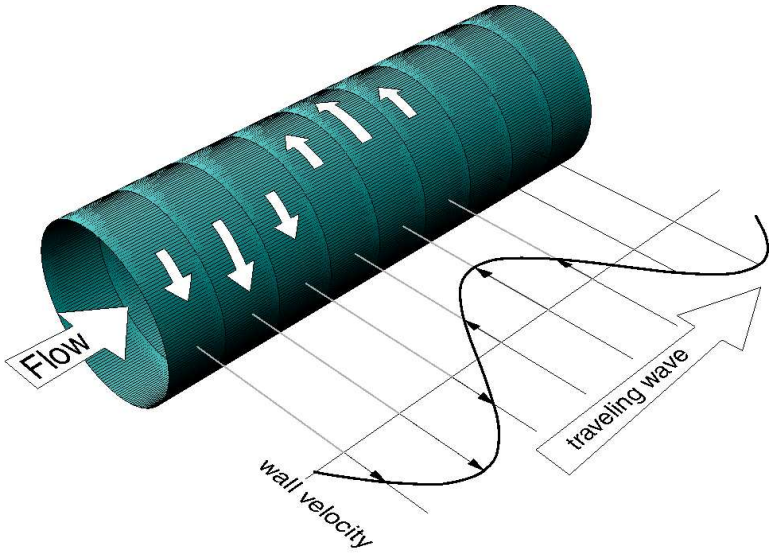

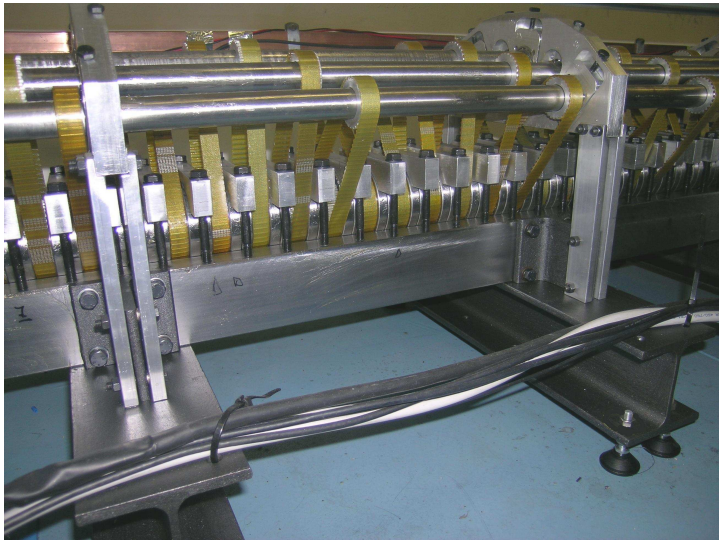

Cylindrical coordinates

- Several problems are usefully set in cylindrical coordinates, for instance: drag reduction experiment (Auteri, Baron, Belan, Campanardi, Quadrio, Phys. Fluids 2010)

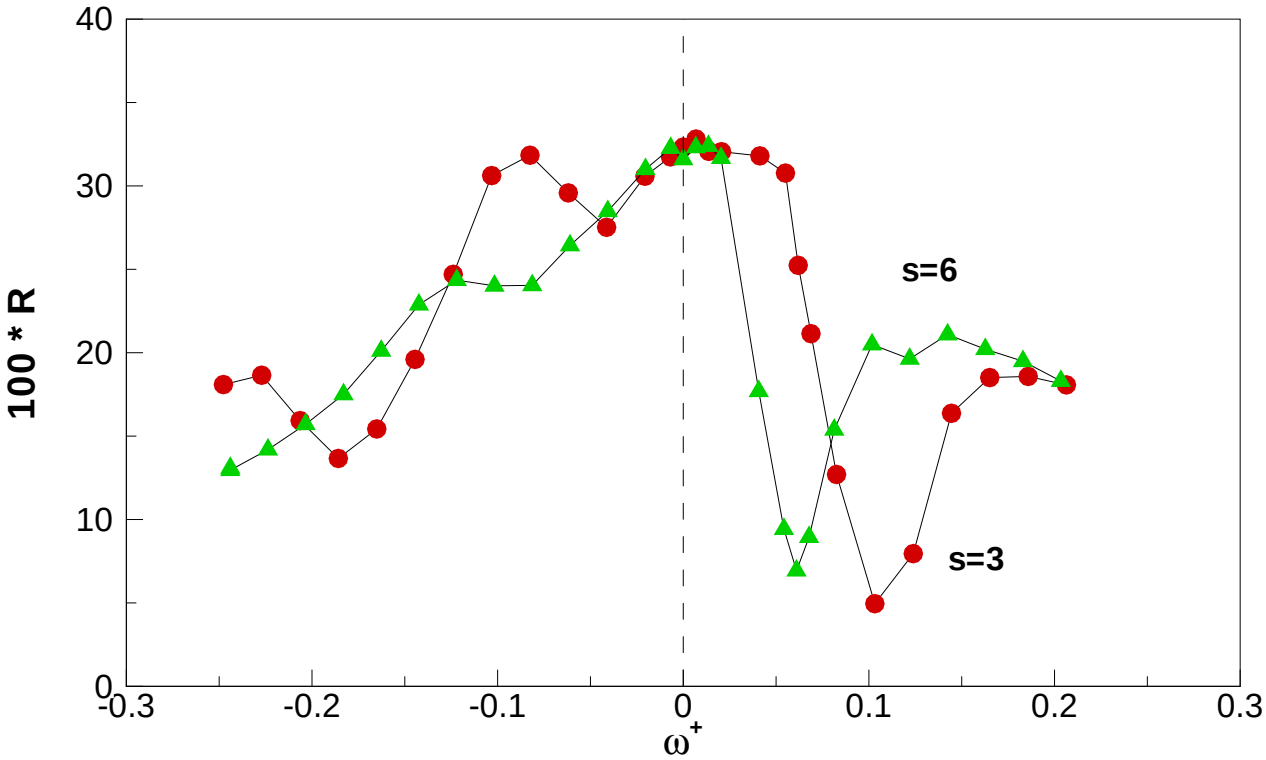

The mathematical problem

The Navier–Stokes equations

$$\begin{cases} \dfrac{\partial \mathbf{u}}{\partial t} + (\mathbf{u}\cdot\boldsymbol{\nabla})\mathbf{u} - \nu\nabla^2\mathbf{u} + \boldsymbol{\nabla} p = \mathbf{f}(\mathbf{r},t), \qquad \boldsymbol{\nabla}\cdot\mathbf{u} = 0, \\ \mathbf{u}_{|\partial\Omega} = \mathbf{b}, \qquad \mathbf{u}_{|t=0} = \mathbf{u}_0, \end{cases}$$

discretized by a semi-implicit 2^{nd}-order projection method

$$\begin{cases} \dfrac{3\mathbf{u}^{k+1} - 4\mathbf{u}^{k} + \mathbf{u}^{k-1}}{2\Delta t} - \nu\,\nabla^2\mathbf{u}^{k+1} = \mathbf{f}^{k+1} - \boldsymbol{\nabla} p^{k}_{\star} - (\mathbf{u}^{k+1}_{\star}\cdot\boldsymbol{\nabla})\mathbf{u}^{k+1}_{\star}, \\ \mathbf{u}^{k+1}{}_{|\partial\Omega} = \mathbf{b}^{k+1} \\ \\ -\nabla^2(p^{k+1} - p^{k}) = -\dfrac{3}{2\Delta t}\,\boldsymbol{\nabla}\cdot\mathbf{u}^{k+1}, \quad \partial_n(p^{k+1} - p^{k})\big|_{\partial\Omega} = 0, \end{cases}$$

Each time step $\rightarrow$ one vector and one scalar elliptic problem.

The solution procedure

Solution steps:

- Fourier transform in the azimuthal ϕ direction $\rightarrow$ sequence of 2D problems;
- uncouple the radial and azimuthal components in the vector problem by similarity transformation;

$$\mathbf{Q}(-\boldsymbol{\partial}_m^2 + \gamma)\,\mathbf{Q} \quad \mathbf{Q}\mathbf{u}_m = \mathbf{Q}\mathbf{f}_m$$

$$\begin{pmatrix} -\partial_{m-1}^2 + \gamma & 0 & 0 \\ 0 & -\partial_{m+1}^2 + \gamma & 0 \\ 0 & 0 & -\partial_m^2 + \gamma \end{pmatrix} \begin{pmatrix} u_{m-1}^1 \\ u_{m+1}^2 \\ u_m^z \end{pmatrix} = \begin{pmatrix} f_{m-1}^1 \\ f_{m+1}^2 \\ f_m^z \end{pmatrix}$$

- discretize the scalar 2D problems by a suitable basis
- solve

Which basis? The centre problem

Cylindrical coordinates are tricky: centre problem

"... the flow solver exhibits a high sensitivity to temporal instability... The resultant stringent stability criteria introduce an upper bound to the Reynolds number and thereby restrict the range of application of the numerical code to the laminar flow regime."
(M. Speetjens, Three-dimensional chaotic advection in a cylindrical domain, Ph.D. Thesis, TU Eindhoven, 2001.)

Lesson

Unwanted resolution near the centre $\Rightarrow$ unduly small time step

Our approach

Satisfy constraints exactly: $u_m(r,z) = r^{|m|} f_m(r^2,z)$ [Lewis & Bellan, 1990] and avoid over-resolution on the axis.

The proposed basis

Matsushima & Marcus, 1995: $Q_n^m(1,1,r) = \rho^m \, P_n^{(0,m)}\left(2\rho^2 - 1\right)$ Problems:

- condition number of typical elliptic operators grows as M^4.
- not convenient to impose Dirichlet b.c.

Mimick Heinrics, 1989, and Shen, 1995:

$$u_{\pm m}(\rho,\zeta) = \sum_{i=m}^{M} \sum_{j=0}^{J} \rho^m \, P_{i-m}^{\star\, m}\left(2\rho^2 - 1\right) u_{i,j;\,\pm m} \, L_j^*(\zeta)$$

where $P_0^{\star\, m}(s) = 1$ and $P_k^{\star\, m}(s) = \dfrac{1-s}{2} \, P_{k-1}^{(1,m)}(s)$, $k = 1, 2, \ldots$

Basis properties

1. It's a basis for $H_0^1(\Omega)$;
2. Diagonal stiffness D and tridiagonal mass M (radial direction);
3. Diagonal stiffness and pentadiagonal mass M (axial direction);
4. Better conditioned discrete operators.

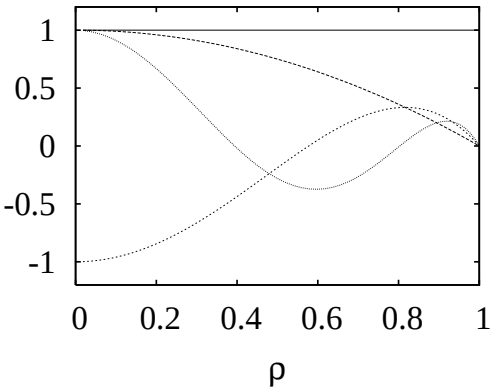

$m = 0$

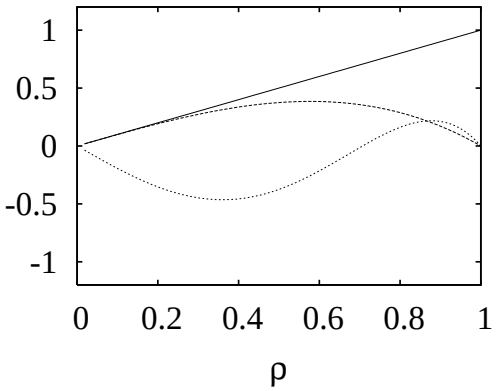

$m = 1$

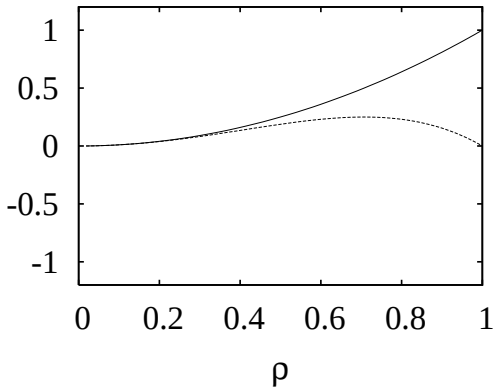

$m = 2$

Basis properties

1. It's a basis for $H_0^1(\Omega)$;
2. Diagonal stiffness D and tridiagonal mass M (radial direction);
3. Diagonal stiffness and pentadiagonal mass M (axial direction);
4. Better conditioned discrete operators.

$$D_{m;\,i,i} = \begin{cases} m, & i = 0 \\ \frac{2i^2}{2i+m}, & i \geq 1 \end{cases}$$

$$M_{m;\,i,i} = \begin{cases} \frac{1}{2(m+1)}, & i = 0 \\ \frac{i^2}{(2i+m-1)(2i+m)(2i+m+1)}, & i \geq 1 \end{cases}$$

$$M_{m;\,i,i+1} = \begin{cases} \frac{1}{2(m+1)(m+2)}, & i = 0 \\ \frac{-i(i+1)}{2(2i+m)(2i+m+1)(2i+m+2)}, & i \geq 1 \end{cases}$$

Basis properties

1. It's a basis for $H_0^1(\Omega)$;
2. Diagonal stiffness D and tridiagonal mass M (radial direction);
3. Diagonal stiffness and pentadiagonal mass M (axial direction);
4. Better conditioned discrete operators.

$$D = \begin{pmatrix} 0 & & & & \\ & 1 & & & \\ & & 1 & & \\ & & & \ddots & \\ & & & & 1 \end{pmatrix} \qquad M = \begin{pmatrix} c_0 & 0 & a_0 & & & \\ 0 & c_1 & 0 & a_1 & & \\ a_0 & 0 & \ddots & 0 & \ddots & \\ & a_1 & 0 & \ddots & 0 & a_{N-2} \\ & & \ddots & 0 & \ddots & 0 \\ & & & a_{N-2} & 0 & c_N \end{pmatrix}$$

$$a_0 = \sqrt{\tfrac{2}{3}},\ a_1 = \tfrac{1}{3\sqrt{5}},\ a_n = \frac{-1}{(2n+1)\sqrt{(2n-1)(2n+3)}},\ n \geq 2,$$
$$c_0 = 2,\ c_1 = \tfrac{1}{3},\ c_n = \frac{2}{(2n-3)(2n+1)},\ n \geq 2.$$

Basis properties

1. It's a basis for $H_0^1(\Omega)$;
2. Diagonal stiffness D and tridiagonal mass M (radial direction);
3. Diagonal stiffness and pentadiagonal mass M (axial direction);
4. Better conditioned discrete operators.

Theorem (Auteri & Quartapelle)
The maximum condition number of the matrices $A_m = D_m + \gamma M_m$, $m \geq 0$, is bounded from above by CN^2 as $N \to \infty$, where $C > 1/2$ is a constant independent of γ.

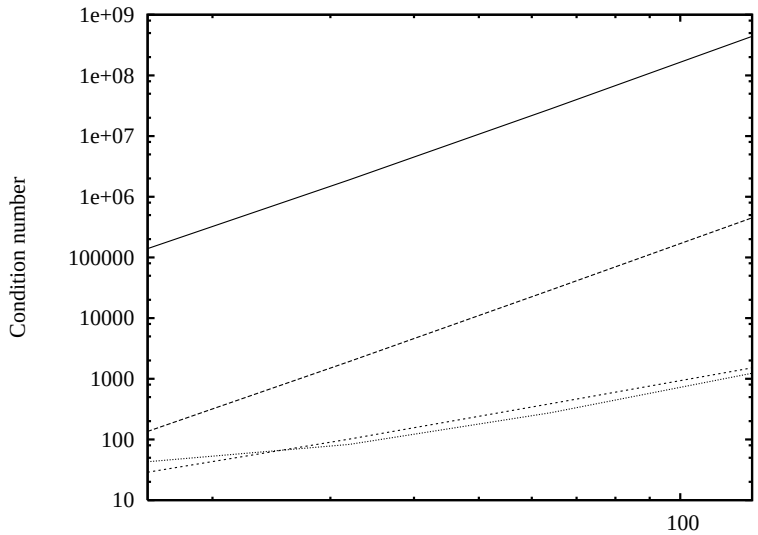

Scalar solver: discrete problem

- Rewrite equations in weak form
- apply Galerkin method to obtain a discrete problem

$$\left(D_m^r + \gamma M_m^r\right) U_m M + M_m^r U_m D = G_m + \langle \text{B.I.} \rangle_m$$

- matrices of decreasing order as m grows from 0 to truncation

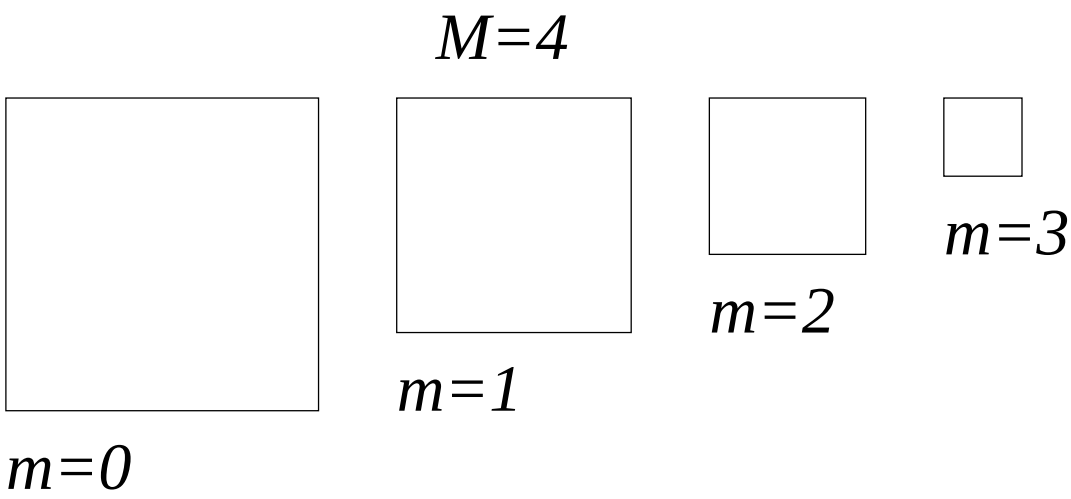

Results: Hopf bifurcation in a cylindrical cavity

Height/radius $= 1.72$, $\mathrm{Re} = 4500$
Bifurcation development

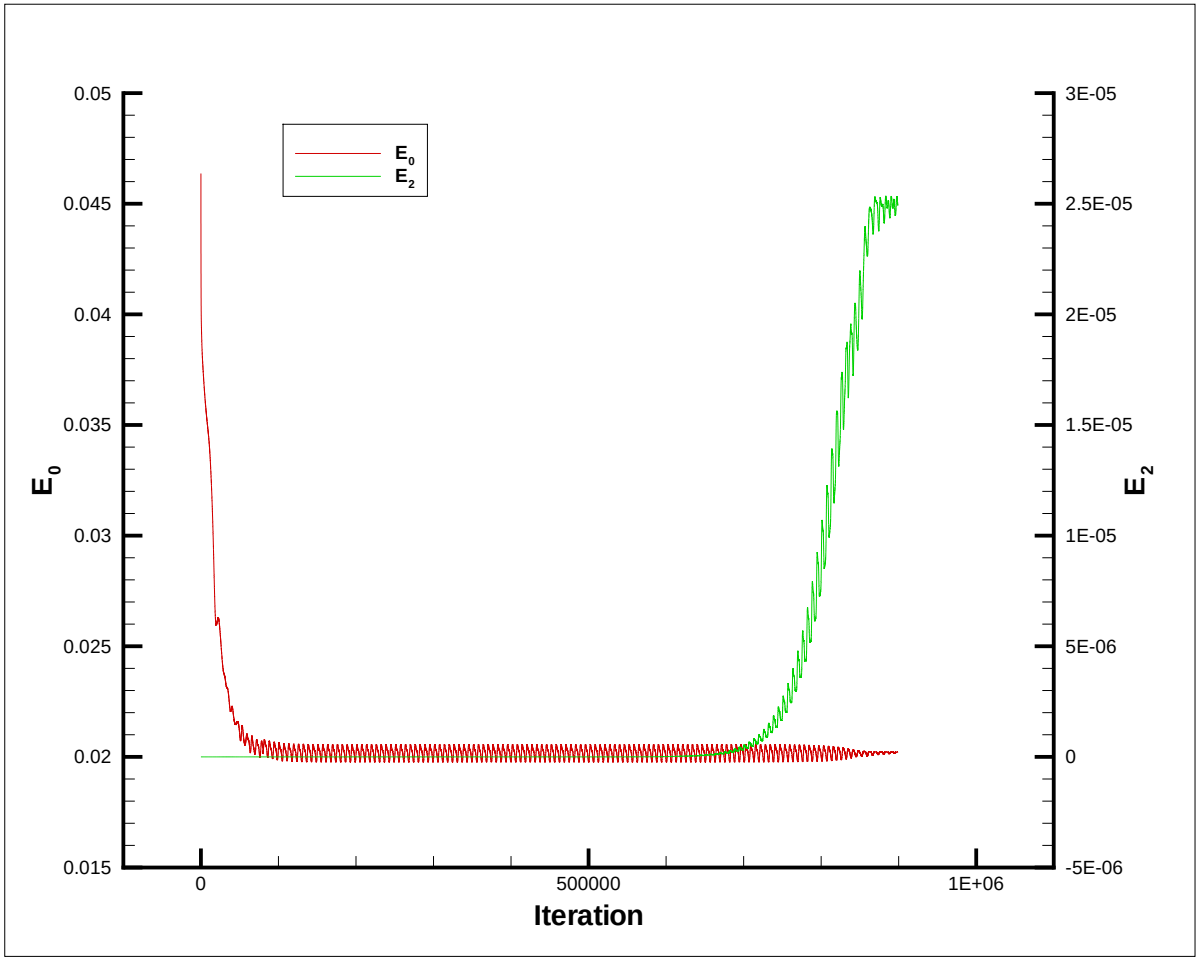

Results: Hopf bifurcation in a cylindrical cavity

Height/radius $= 1.72$, $\mathrm{Re} = 4500$
Bifurcation development: zoom

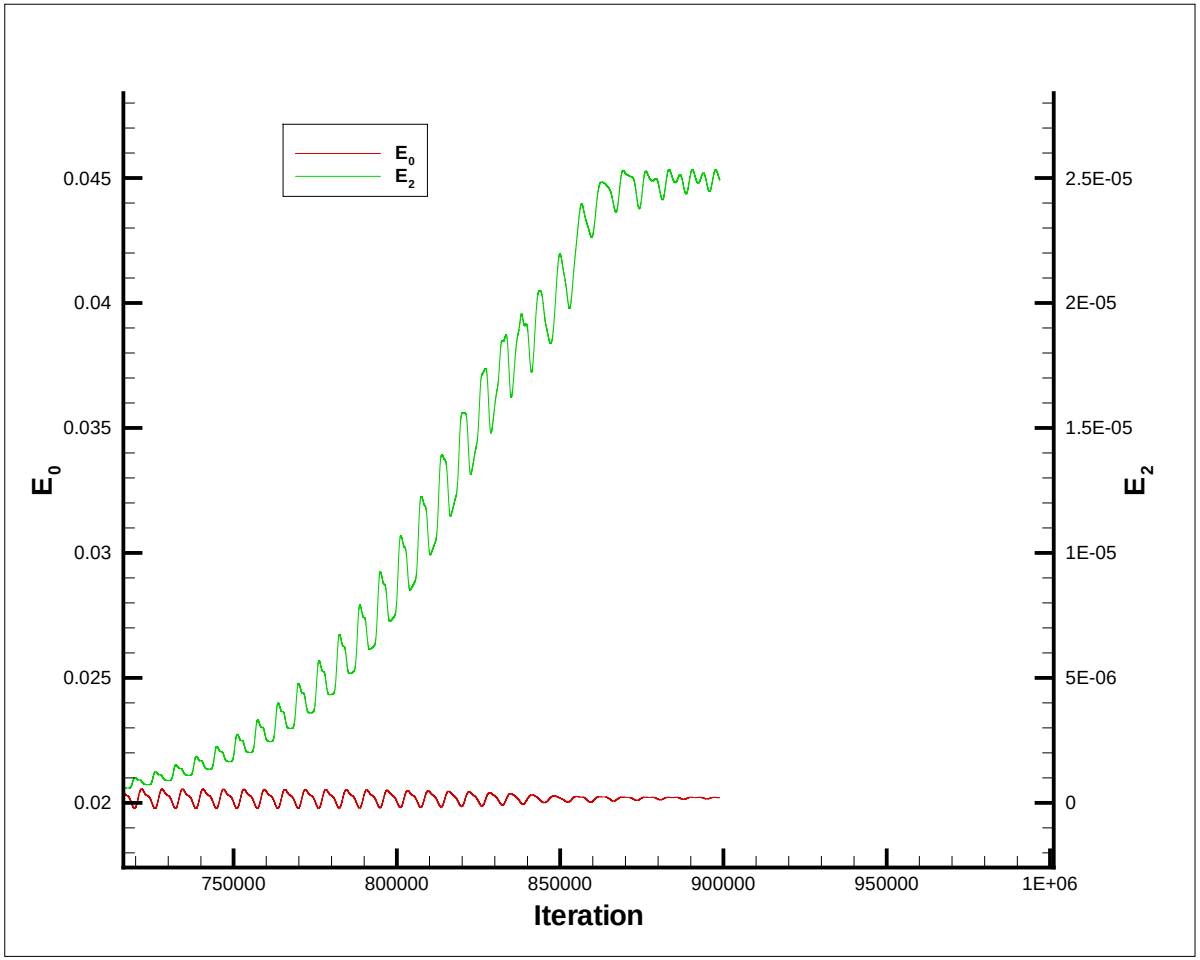

Results: Hopf bifurcation in a cylindrical cavity

u_r

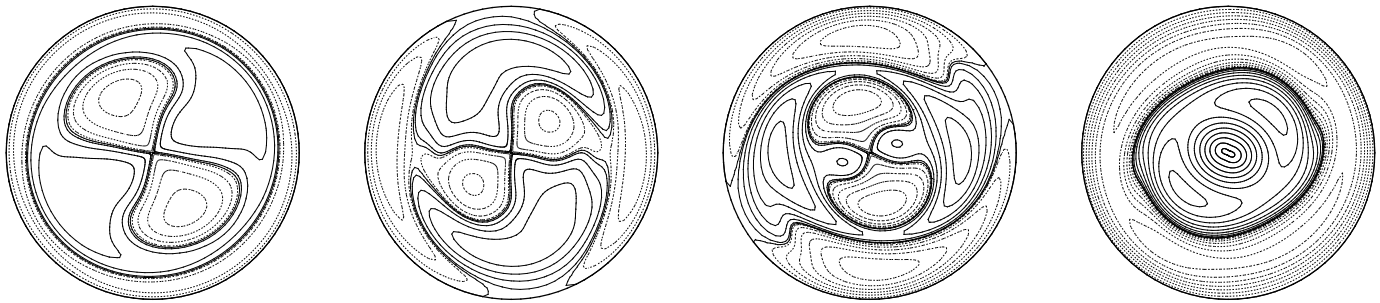

u_θ

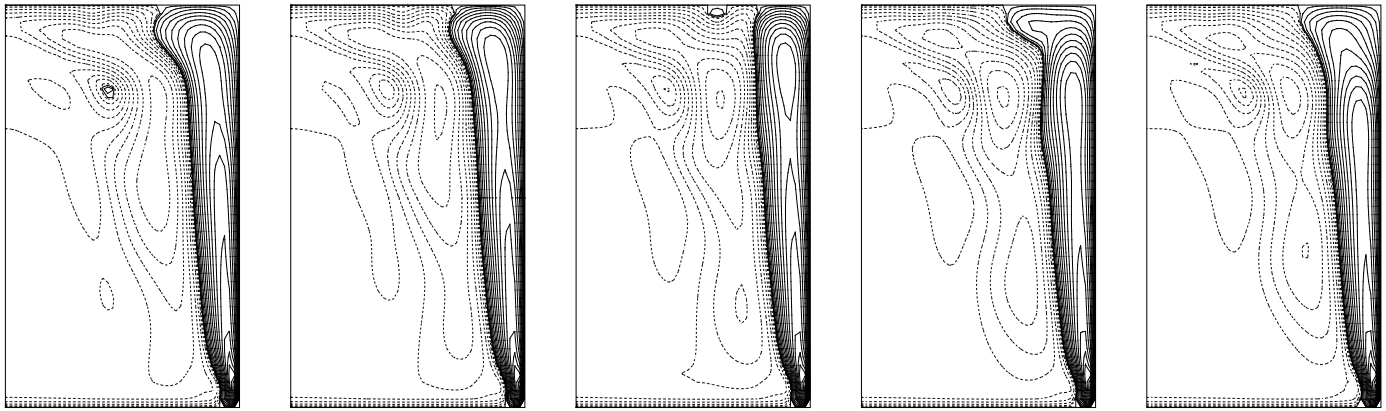

Results: cylindrical GSL thickness (Re= 4900)

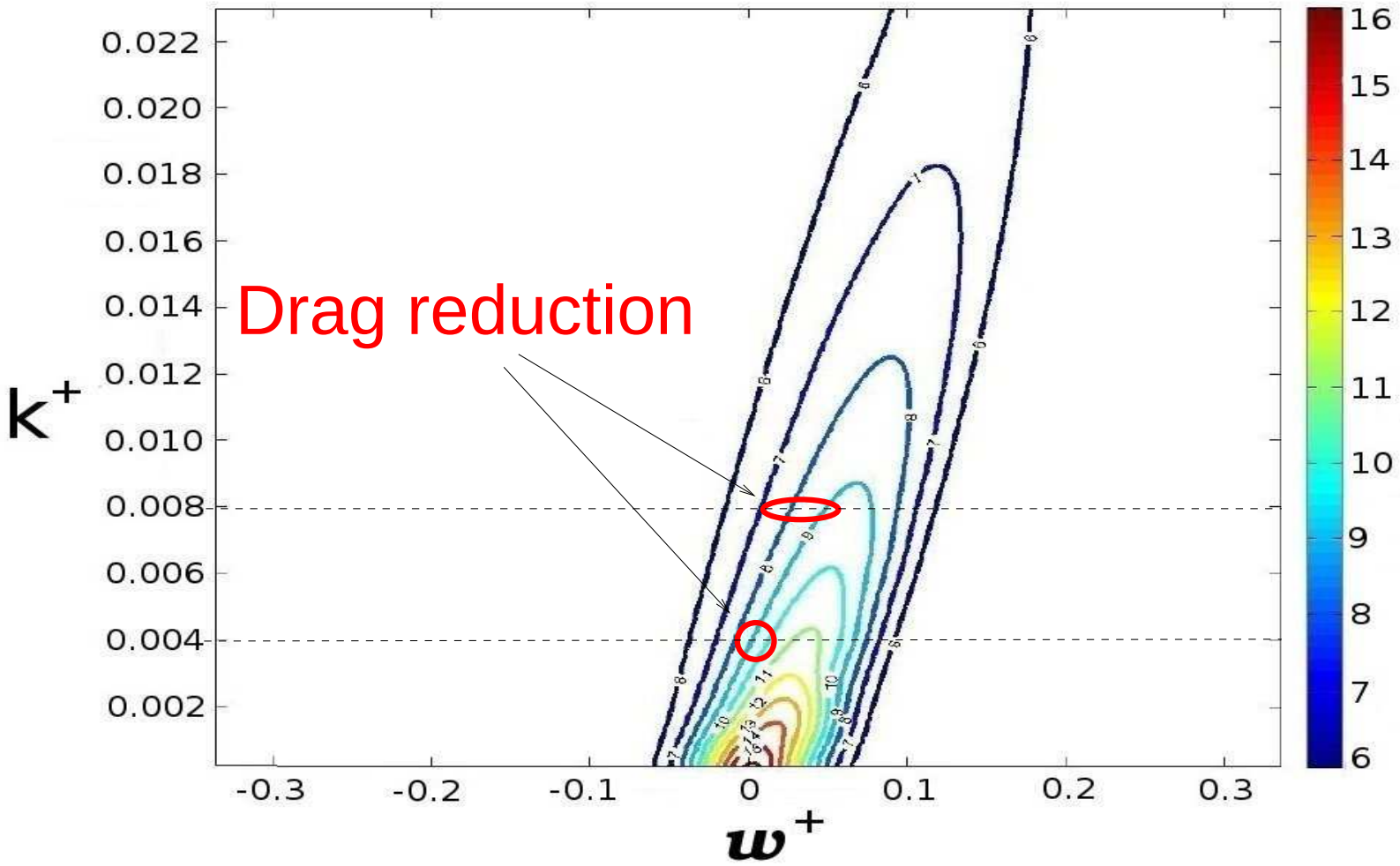

Sphere: motivation

The sphere:

1. Simplest geometry, no singularities;
2. Study effects of rotation and symmetries on transition and turbulence;
3. Applications: flow in eyes, simple framework for MHD studies.

Example: desktop turbulence generator (Goto & Kida experiment)

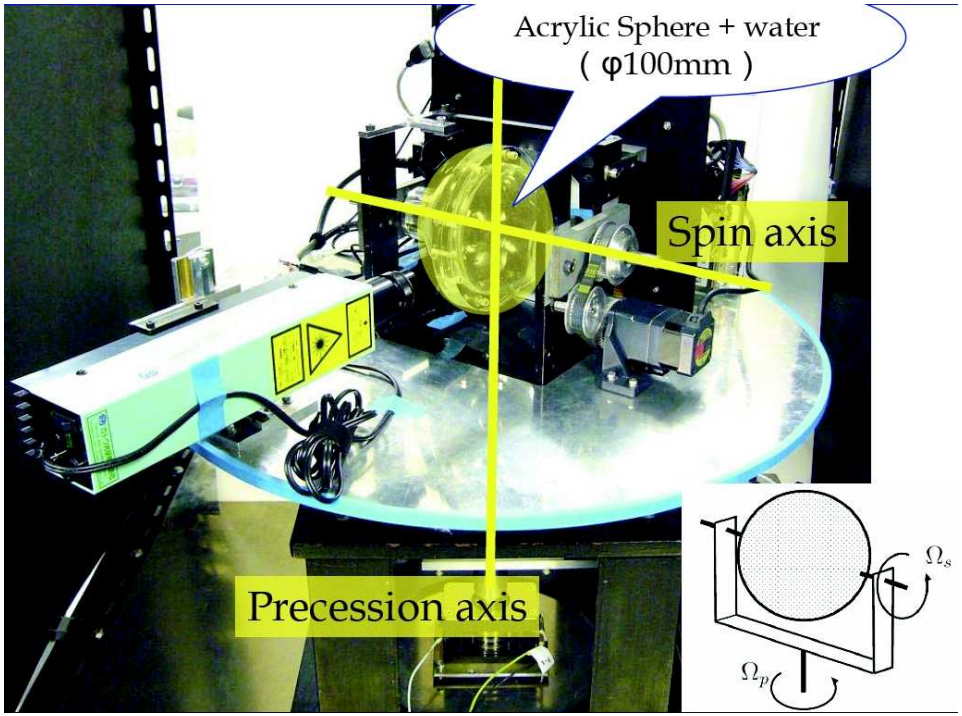

Equations, ϕ discretization and uncoupling

We want to solve the unsteady incompressible Navier–Stokes equations.

1. Discretization in time: semi-implicit second order projection method
2. Longitude discretization: Fourier expansion

$$\mathbf{u}(r,\theta,\phi) = \mathbf{u}^0(r,\theta) + 2\sum_{m=1}^{N-1}\left[\mathbf{u}^m(r,\theta)\cos(m\phi) - \mathbf{u}^{-m}(r,\theta)\sin(m\phi)\right].$$

3. Uncoupling: variable transformation, uncoupled ellipti problems:c

$$\left(-\partial_m^2 + \gamma\right) u^m = f^m(r,\theta),$$

Discretization: θ and r

1. Associate Legendre functions:

$$u^m(r,\theta) = \sum_{\ell=|m|}^{N} u_\ell^m(r)\, \hat{P}_\ell^{|m|}(\cos\theta), \hat{P}_\ell^m(z) \equiv \sqrt{\frac{2\ell+1}{2}\frac{(\ell-m)!}{(\ell+m)!}}\, P_\ell^m(z).$$

2. $\rightarrow$ uncoupled ODE with Dirichlet ($\mathbf{u}$) or Neumann (p) condition

$$\int_0^1 v\left\{-\frac{d}{dr}\left(r^2\frac{du_\ell^m}{dr}\right) + \left[\ell(\ell+1)+\gamma r^2\right] u_\ell^m\right\} dr = \int_0^1 r^2\, v(r)\, f_\ell^m(r)\, dr,$$

3. Suitable Jacobi polynomial basis

$$u_\ell^m(r) = \sum_{i=0}^{N-\ell} u_i^{\ell,m}\, B_i^\ell(r), B_i^\ell(r) = \begin{cases} r^\ell & i=0, \\ \left(1-r^2\right) r^\ell\, P_{i-1}^{(1,\ell+\frac{1}{2})}\left(2r^2-1\right) & i \geq 1. \end{cases}$$

1D discrete problems

The linear system becomes

$$\left(D^{\ell} + \gamma M^{\ell}\right) u^{\ell,\,m} = f^{\ell,\,m},$$

where

$$D^{\ell}_{i,i'} = \int_{-1}^{1} \left\{ 4\left(\frac{1+s}{2}\right)^{\frac{3}{2}} \frac{dQ^{\ell}_{i}(s)}{ds} \frac{dQ^{\ell}_{i'}(s)}{ds} + \frac{\ell(\ell+1)}{4}\left(\frac{1+s}{2}\right)^{-\frac{1}{2}} Q^{\ell}_{i}(s)\, Q^{\ell}_{i'}(s) \right\} ds,$$

$$M^{\ell}_{i,i'} = \frac{1}{4}\int_{-1}^{1} \left(\frac{1+s}{2}\right)^{\frac{1}{2}} Q^{\ell}_{i}(s)\, Q^{\ell}_{i'}(s)\, ds, \quad 0 \leq (i, i') \leq N - \ell.$$

1D discrete problems

First result:

M^ℓ is tridiagonal (and symmetric)

$$M^\ell_{i,i} = \begin{cases} \dfrac{1}{2\ell+3} & \text{for } i = 0, \\ \dfrac{i^2}{\left(2i+\ell-\frac{1}{2}\right)\left(2i+\ell+\frac{1}{2}\right)\left(2i+\ell+\frac{3}{2}\right)} & \text{for } i \geq 1, \end{cases}$$

$$M^\ell_{i,i+1} = \begin{cases} \dfrac{2}{(2\ell+3)(2\ell+5)} & \text{for } i = 0, \\ \dfrac{-i(i+1)}{2\left(2i+\ell+\frac{1}{2}\right)\left(2i+\ell+\frac{3}{2}\right)\left(2i+\ell+\frac{5}{2}\right)} & \text{for } i \geq 1. \end{cases}$$

1D discrete problems

Second result:

D^ℓ is diagonal

$$D^\ell_{i,i} = \begin{cases} \ell & \text{for } i = 0, \\ \dfrac{2i^2}{2i + \ell + \frac{1}{2}} & \text{for } i \geq 1 \end{cases}$$

Conditioning results

Third result: the linear systems are well conditioned

Theorem
There exists a constant C independent of γ and of N such that the maximum condition number of $D^\ell + \gamma M^\ell$ is bounded from above by CN^2.

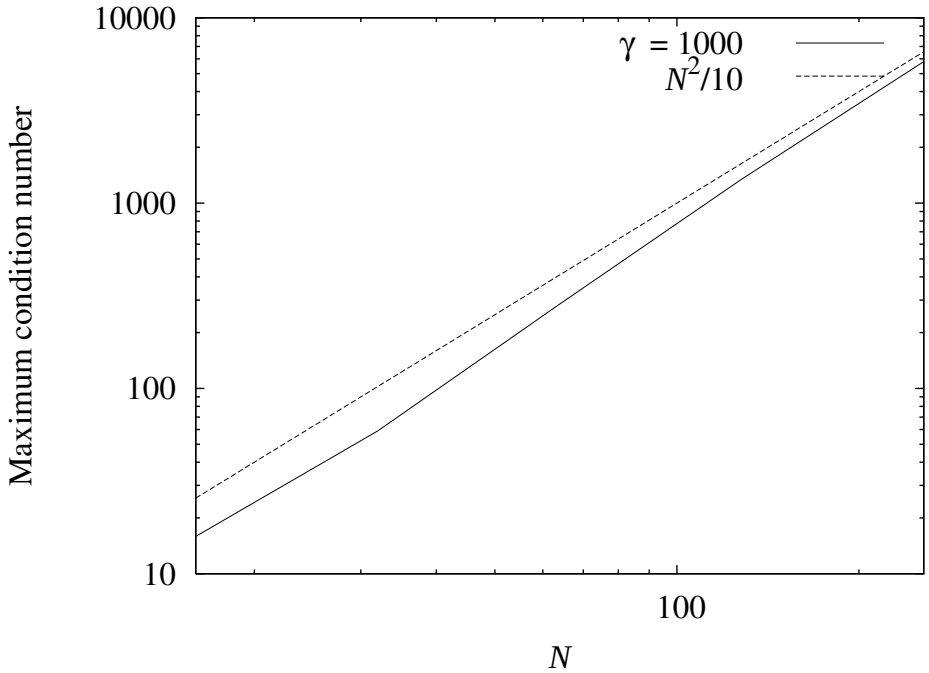

Convergence results

Providing LBB condition is satisfied, we obtain

Spectral accuracy in space

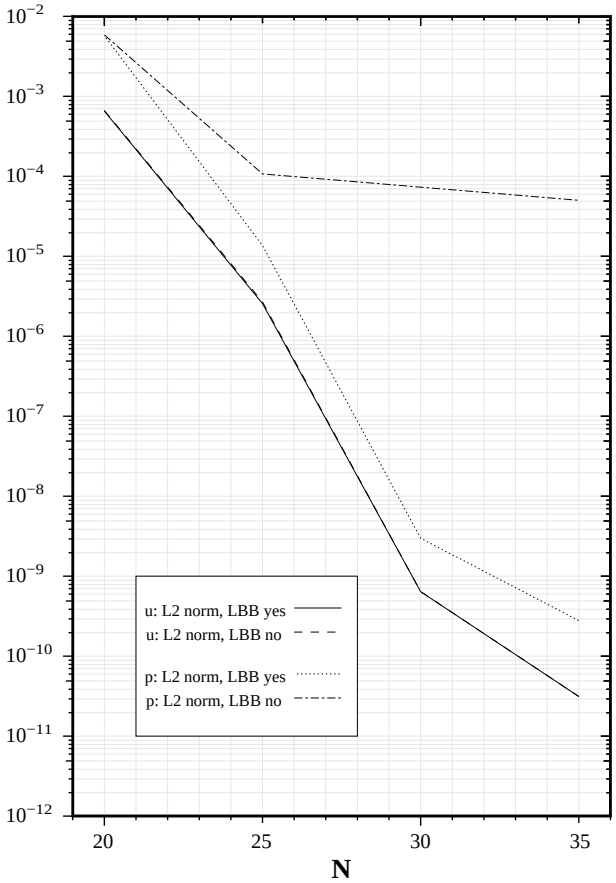

Second order accuracy in time

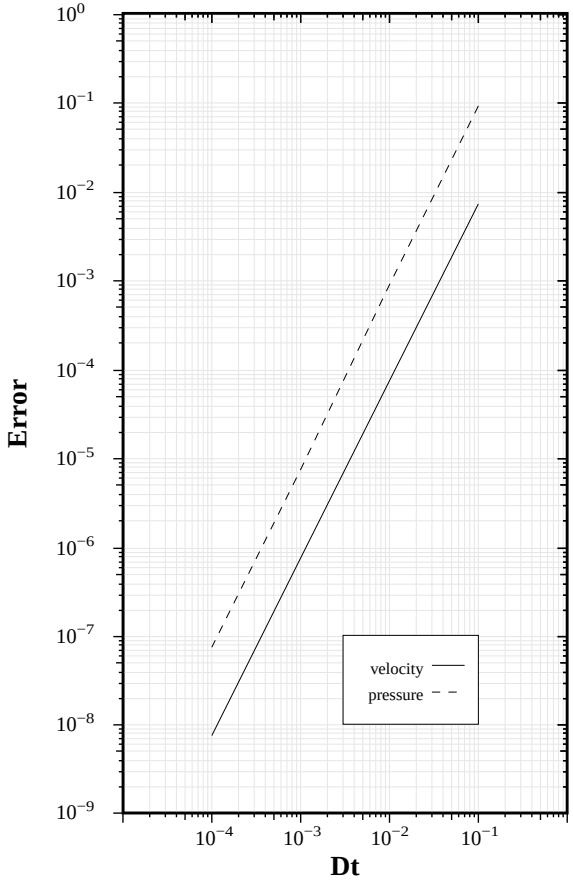

Unsteady simulations: precessing sphere

Hopf bifurcation. Computation parameters: $\mathrm{Re} = 1650$, $\Gamma = 0.1$. Normal component of the velocity.

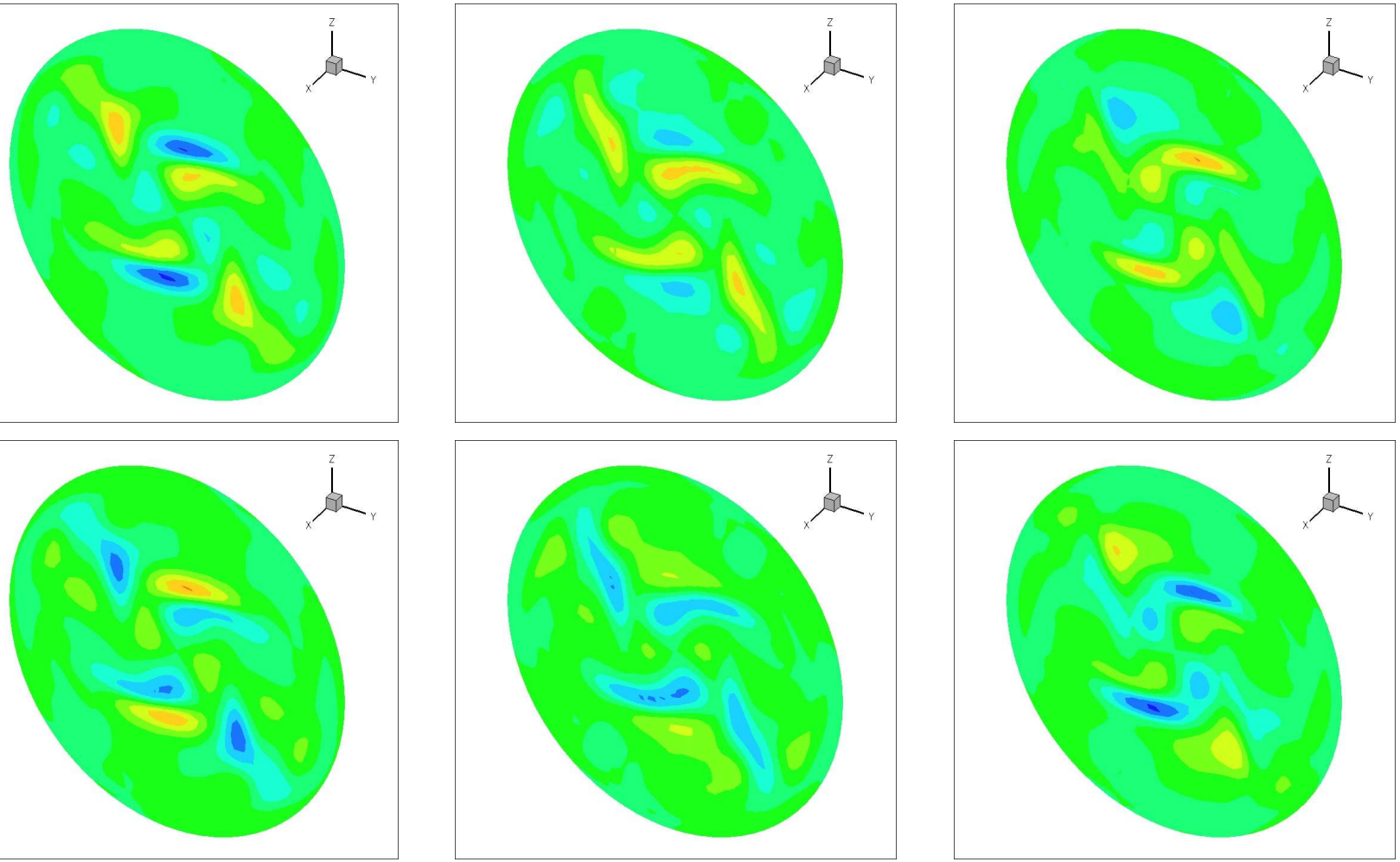

The steady solver

1. Fact: the unsteady solver is not efficient to solve for the base flow (linear stability problem).
2. A preconditioned Newton–Krylov could be built.
3. What preconditioner? We can build a direct Stokes solver using integral pressure conditions (Quartapelle & Verri, 1995)!
4. The same direct Stokes solver allows us to build a divergence free Krylov subspace and to get rid of pressure in the Krylov iteration.

The direct Stokes solver

1. The Stokes–Dirichlet problem: $-\nabla^2 \mathbf{u} + \boldsymbol{\nabla} p = \mathbf{f}$, $\boldsymbol{\nabla} \cdot \mathbf{u} = 0$, $\mathbf{u}_{|\Gamma} = \mathbf{b}$.
2. Difficult step: compute pressure, trivial step: compute velocity.
3. First: obtain a pressure equation with integral pressure conditions:

$$\nabla^2 p = \boldsymbol{\nabla} \cdot \mathbf{f}, \quad \int_\Omega \boldsymbol{\nabla} p \cdot \boldsymbol{\eta} = \int_\Omega \mathbf{f} \cdot \boldsymbol{\eta} - \oint_\Gamma (\mathbf{n} \cdot \mathbf{b}\, \boldsymbol{\nabla} \cdot \boldsymbol{\eta} + \mathbf{n} \times \mathbf{b} \cdot \boldsymbol{\nabla} \times \boldsymbol{\eta})$$

   where $\boldsymbol{\eta}$ are vector harmonic functions satisfying $\mathbf{n} \times \boldsymbol{\eta}_{|\Gamma} = 0$, known in closed form.
4. Second: expand p, discretize by Galerkin method $\rightarrow$ trivial linear systems.
5. Compute the right hand side expanding $\mathbf{f}$ in vector spherical harmonics.
6. Solve for pressure $p \triangleq \mathcal{P}^{\int}_{\mathbf{b}}(\mathbf{f})$, $\mathbf{u} = \boldsymbol{\mathcal{S}}_{\mathbf{b}}(\mathbf{f})$.

The Newton–Krylov solver: algorithm

1. Given an initial guess $(\mathbf{u}_0, p_0)$, set $n = 0$;
2. Up to prescribed tolerance:
   - Solve the linearized (incremental) problem supplemented by homogeneous velocity condition to give

$$\begin{cases} (\mathrm{Re}\mathbf{L}^{\mathbf{u}_n} - \nabla^2)\delta\mathbf{u} + \boldsymbol{\nabla}\delta p = -\mathrm{Re}(\delta\mathbf{u}_n \cdot \boldsymbol{\nabla})\delta\mathbf{u}_n, \\ \boldsymbol{\nabla}\cdot\delta\mathbf{u} = 0, \quad \delta\mathbf{u}_{|\Gamma} = 0. \end{cases}$$

     by a preconditioned Krylov iterative linear solver;
   - Update: $\mathbf{u}_{n+1} = \mathbf{u}_n + \delta\mathbf{u}$, and $p_{n+1} = p_n + \delta p$, $n = n + 1$.

The preconditioned linear solver

We introduce the $\boldsymbol{\mathcal{S}}_0$ operator "vector field solution of the homogeneous Stokes problem". Then the algorithm reads

1. Right-hand side projection and preconditioning : $\mathbf{h} = \boldsymbol{\mathcal{S}}_0 \, \mathbf{g}$
2. Initialize solver with $\mathbf{h}$; until convergence when solver asks for matrix multiplication times $\mathbf{w}$:
   - compute $q = -\mathrm{Re}\mathcal{P}_0^{\int}(\mathbf{L^a w})$
   - return the solution of the homogeneous Stokes problem: $\delta\mathbf{u}^k = \boldsymbol{\mathcal{S}}_0 \left(\mathrm{Re}\mathbf{L^a w} - \nabla^2 \mathbf{w} + \boldsymbol{\nabla} q\right)$

Efficiency and convergence results

The preconditioner is optimal with respect to discretization (but not with respect to Reynolds number).

N	8	12	16	20	24
It. no preconditioning	505	625	643	692	744
It. Preconditioning	158	159	159	159	160

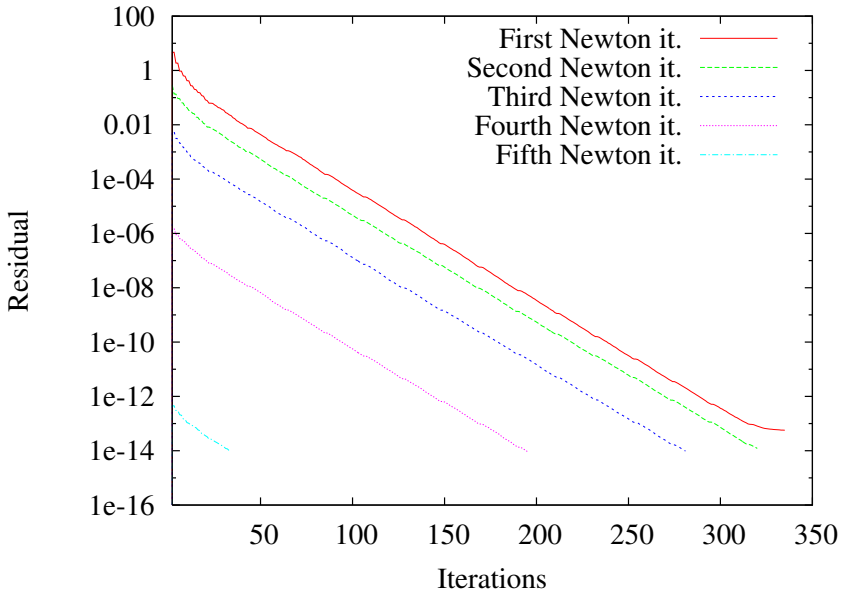

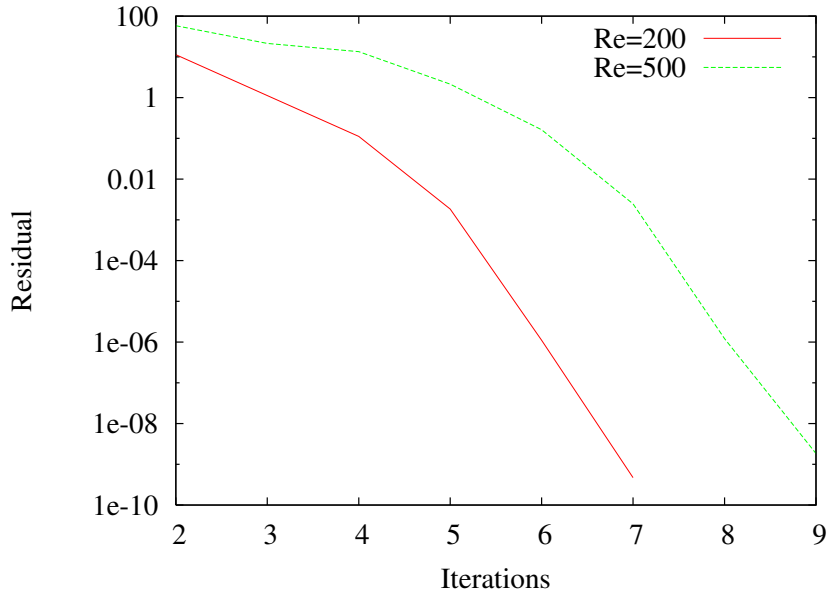

Results: precessing sphere Re= 500

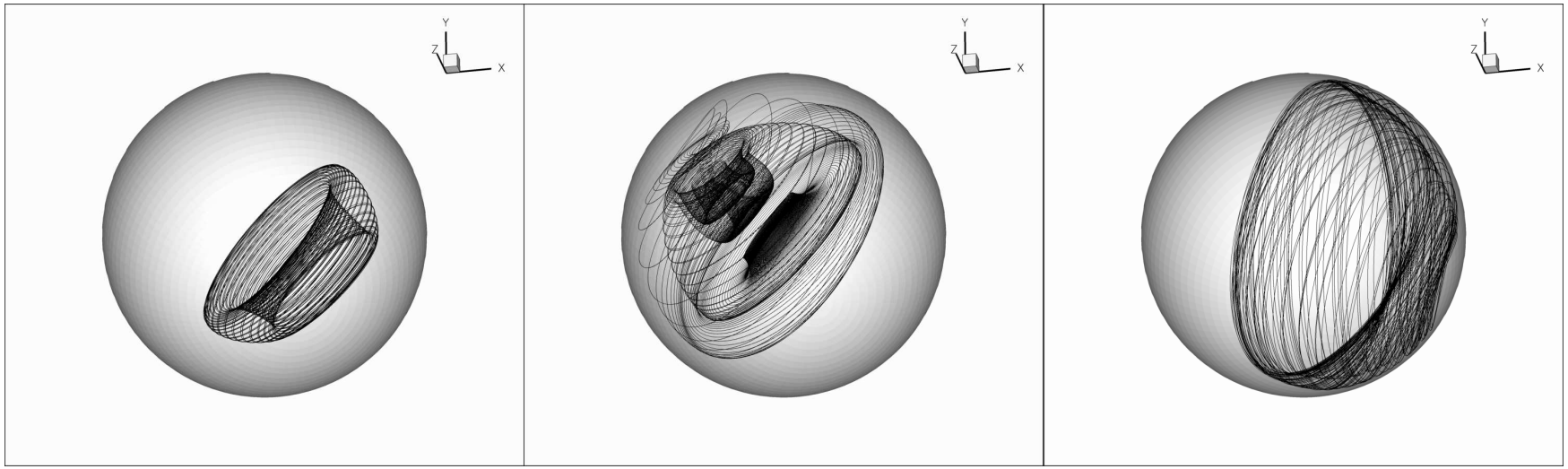

Outline

Laguerre spectral methods for boundary layer external flows

(collaboration with L. Quartapelle)

Motivation: transition control and drag reduction

Growing interest in transition control and turbulent friction drag reduction.
Questions

1. How do some flow control techniques really work?
2. Do they are effective to delay transition?
3. How are they affected by Reynolds number, accelerating/decelerating flow, three-dimensionality?

Need for reliable and efficient boundary layer solvers.

Preliminaries: a Falkner–Skan–Cooke–Orr–Sommerfeld solver (1D)

1. Goal: test Laguerre spectral methods on a non-trivial problem;
2. Useful as a reference for stability, despite parallel flow approximation is introduced;
3. Useful to compute perturbations to initial and boundary conditions.

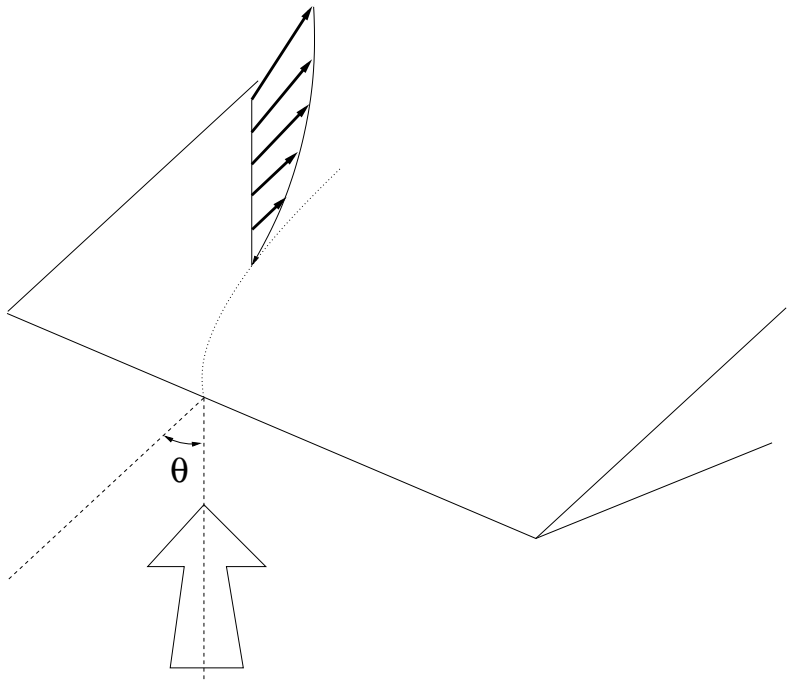

Equations and boundary conditions

Falkner–Skan–Cooke

$$f''' + \alpha f f'' + \beta\left[1 - (f')^2\right] = 0, \quad f(0) = 0, \quad f'(0) = 0, \quad \lim_{\eta\to\infty} f'(\eta) = 1,$$

$$g'' + \alpha f(\eta)\, g' = 0, \qquad g(0) = 0 \quad \text{and} \quad \lim_{\eta\to\infty} g(\eta) = 1.$$

Orr–Sommerfeld–Squire (parallel flow approximation)

$$\begin{cases} \dfrac{1}{\mathrm{Re}_\theta}\left(v'''' - 2k^2 v'' + k^4 v\right) - \mathrm{i}\,\dfrac{\partial}{\partial\eta}\left[\mathcal{S}_\theta(\eta,\alpha,\beta)\, v' - \dfrac{\partial \mathcal{S}_\theta(\eta,\alpha,\beta)}{\partial\eta}\, v\right] \\ \qquad\qquad + \mathrm{i}\, k^2 \mathcal{S}_\theta(\eta,\alpha,\beta)\, v = \mathrm{i}\, c\alpha\left(-v'' + k^2 v\right), \\ \dfrac{1}{\mathrm{Re}_\theta}\left(-\omega'' + k^2\omega\right) + \mathrm{i}\,\mathcal{S}_\theta(\eta,\alpha,\beta)\,\omega = \mathrm{i}\, c\alpha\omega - \mathrm{i}\,\beta[f''(\eta) - g'(\eta)]\, v, \end{cases}$$

Laguerre basis functions: different strategies for different equations

Falkner–Skan:

1. change of variables to simplify the problem;
2. test and trial functions for the biharmonic problem (Shen, 2000);
3. perturb one trial function to accommodate a non-trivial constant asymptotic behaviour (Petrov–Galerkin).

Cooke:

1. change of variables to simplify the problem;
2. same second-order Laguerre basis for trial and test functions;

Orr–Sommerfeld–Squire:

1. no need for a change of variables;
2. biharmonic Laguerre basis for the normal velocity, second-order Laguerre basis for normal vorticity;

Basis functions

FS test	FS trial	Cooke	OS v	OS ω
$\mathcal{C}_i(\eta)$ $i = 1, 2, \ldots$	$\mathcal{C}_i^\star(\eta)$ $i = 1, 2, \ldots$	$\mathcal{B}_i(\eta)$ $i = 1, 2, \ldots$	$\mathcal{C}_i(\eta)$ $i = 2, 3, \ldots$	$\mathcal{B}_i(\eta)$ $i = 1, 2, \ldots$

where:

$$\mathcal{B}_i(\eta) = \eta e^{-\eta/2} L_{i-1}^{(1)}(\eta)/i$$

$$\mathcal{C}_1(x) = x e^{-x/2},$$

$$\mathcal{C}_i(x) = e^{-x/2}[L_{i-2}(x) - 2L_{i-1}(x) + L_i(x)], \quad i \geq 2,$$

$$\mathcal{C}_1^\star(x) = 1 - \left(1 + \frac{x}{2}\right) e^{-x/2}$$

$$\mathcal{C}_i^\star(x) = \mathcal{C}_i(x), \quad i \geq 2.$$

Falkner–Skan

1. Scaling: $f(\eta) = f(\chi\hat{\eta}) = \hat{f}(\hat{\eta}) = \hat{f}(\eta/\chi)$
2. Change of variable: $\hat{f}(\hat{\eta}) = \hat{\psi}(\hat{\eta}) + \chi\hat{\eta}\left(1 - e^{-\hat{\eta}/2}\right)$
3. To obtain

$$\hat{\psi}''' + \chi\alpha\hat{\psi}\,\hat{\psi}'' - \chi\beta\left(\hat{\psi}'\right)^2 + \chi^2\left[\alpha a(\hat{\eta})\,\hat{\psi}'' + \beta b(\hat{\eta})\,\hat{\psi}' + \alpha c(\hat{\eta})\,\hat{\psi}\right] = \hat{r}(\hat{\eta}),$$

4. and, after Petrov–Galerkin discretization,

$$\hat{L}_\chi^\star\hat{\boldsymbol{\psi}} - \chi\mathbf{nl}(\hat{\psi}) = \hat{\mathbf{r}}.$$

5. Use Newton iteration to solve the nonlinear problem.

Cooke

1. Change of variable: $g(\eta) = \gamma(\eta) + 1 - e^{-\eta/2}$,
2. To obtain
$$\gamma'' + \alpha f(\eta)\,\gamma' = h(\eta),$$
3. and, after Galerkin discretization,
$$\left(-\tilde{D}^2 + \alpha \tilde{F} \right) \boldsymbol{\gamma} = \mathbf{h},$$
4. Solve by Lapack dense linear solver.

Orr–Sommerfeld–Squire

1. Galerkin discretization of Orr–Sommerfeld eigenvalue problem

$$A(\boldsymbol{\alpha}_\diamond, \mathrm{Re}_\theta)\mathbf{v} = cB(\boldsymbol{\alpha}_\diamond, \mathrm{Re}_\theta)\mathbf{v}$$

involving the pair of matrices

$$A(\boldsymbol{\alpha}_\diamond, \mathrm{Re}_\theta) = D^4 + 2\alpha_\diamond^2 D^2 + \alpha_\diamond^4 M + \mathrm{i}\,\mathrm{Re}_\theta\left[N_\theta(\boldsymbol{\alpha}_\diamond) + \alpha_\diamond^2 S_\theta(\boldsymbol{\alpha}_\diamond)\right]$$
$$B(\boldsymbol{\alpha}_\diamond, \mathrm{Re}_\theta) = \mathrm{i}\,\alpha\mathrm{Re}_\theta\left(D^2 + \alpha_\diamond^2 M\right)$$

2. Solve the Squire equation for the normal vorticity

$$\left[\tilde{D}^2 + \alpha_\diamond^2 \tilde{M} + \mathrm{i}\,\mathrm{Re}_\theta \tilde{S}_\theta(\boldsymbol{\alpha}_\diamond)\right]\boldsymbol{\omega}_p = \mathrm{i}\,\mathrm{Re}_\theta \mathbf{r}(\boldsymbol{\alpha}_\diamond),$$

3. Obtain the other velocity components

$$\tilde{M}\mathbf{u} = \mathrm{i}\,\frac{\alpha\mathbf{q} - \beta\mathbf{p}}{\alpha^2 + \beta^2} \qquad \text{and} \qquad \tilde{M}\mathbf{w} = \mathrm{i}\,\frac{\beta\mathbf{q} - \alpha\mathbf{p}}{\alpha^2 + \beta^2},$$

where $q_i = \int_0^\infty \mathcal{B}_i(\eta)\, v'(\eta)\, d\eta$ and $p_i = \int_0^\infty \mathcal{B}_i(\eta)\, \omega_p(\eta)\, d\eta$.

Some results

β	Present $\chi = 0.1$	Asaithambi, 2005
2	1.687218169	1.687218
1	1.232587657	1.232589
0.5	0.927680040	0.927680
-0.1	0.319269760	0.319270
-0.15	0.216361406	0.216361
-0.18	0.128636221	0.128637
-0.1988	0.005218188	0.005225
-0.18^r	-0.097692060	–
-0.15^r	-0.133421238	–
-0.1^r	-0.140546213	–

Falkner–Skan equation, $f''(0)$ value. The apex ^{r} indicates the reversed flow cases

Some results

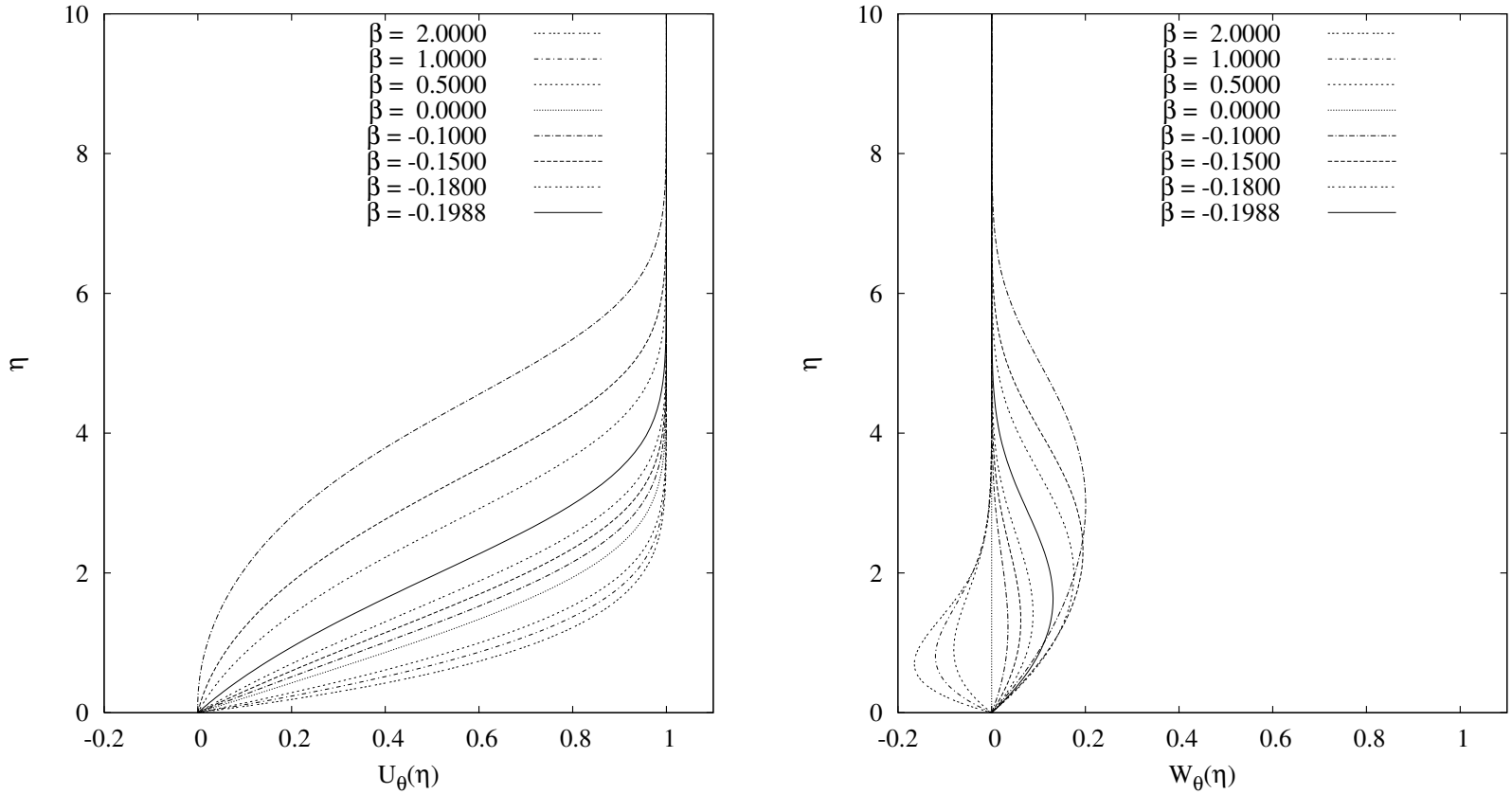

Velocity profiles, Falkner–Skan–Cooke swept b.l. ($\theta = 45°$) Reference system aligned with free stream velocity. Left: longitudinal component. Right: transverse component.

Some results

Neutral-stability curves of two and three-dimensional disturbances, decelerating Falkner–Skan–Cooke b. l. $\theta = 30^\circ$ $\alpha_{\mathrm{FS}} = 1$, $\beta_{\mathrm{FS}} = -0.1$.

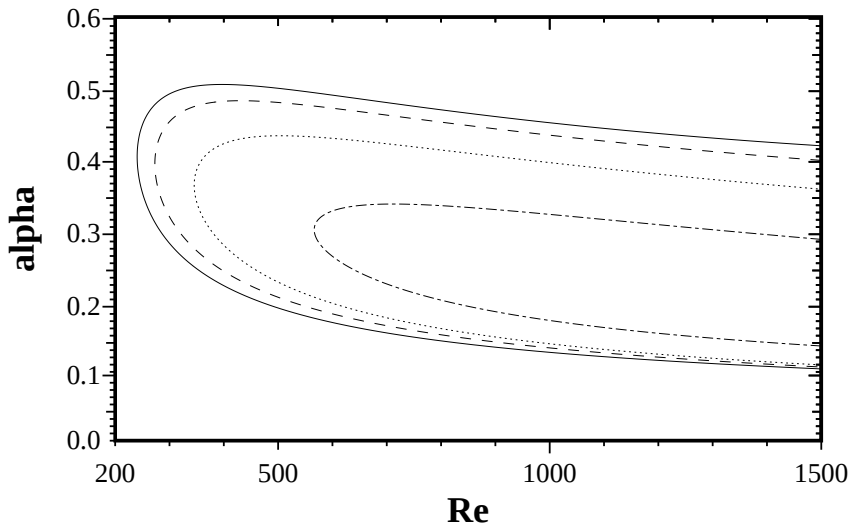

Attached.
Solid: $\beta = 0$.
Dashed: $\beta = 0.1$.
Dotted: $\beta = 0.2$.
Dotted-dashed: $\beta = 0.3$.

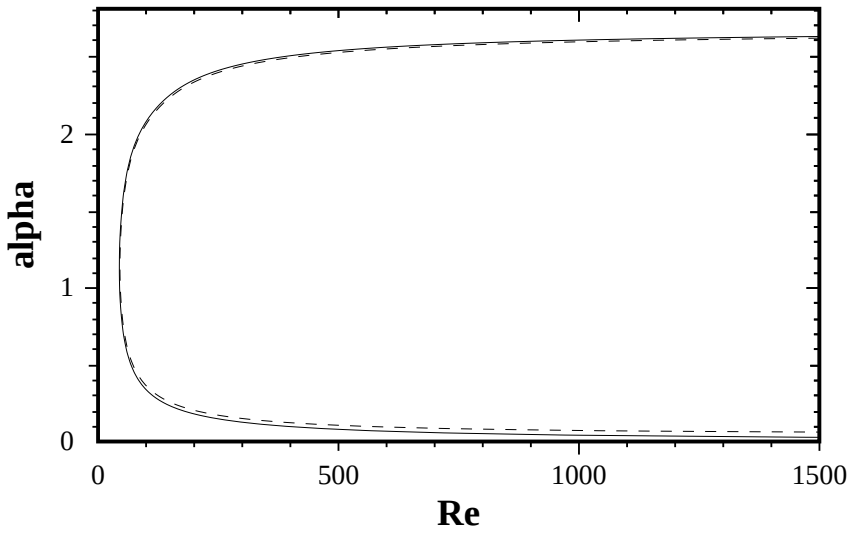

Separated.
Solid line: $\beta = 0$.
Dashed line: $\beta = 0.1$.

3D Navier–Stokes equations

The Navier–Stokes equations uncoupled and discretized in time by a second order projection method (Guermond, 1999)

$$\frac{\mathbf{u}^{k+1} - \mathbf{u}^{k}}{\Delta t} - \nu \nabla^2 \mathbf{u}^{k+1} = \mathbf{f}^{k+1} - (\mathbf{u}_\star^{k+1} \cdot \boldsymbol{\nabla}) \mathbf{u}_\star^{k+1} - \boldsymbol{\nabla} p^{k}, \quad k \geq 1$$

$$-\hat{\nabla}^2 p^{k+1} = -(\Delta t)^{-1} \, \boldsymbol{\nabla} \cdot \mathbf{u}^{k+1}, \quad k \geq 0,$$

where $\mathbf{u}_\star^{k+1} = 2\mathbf{u}^{k} - \mathbf{u}^{k-1}$.

The boundary conditions

1. Plate: no-slip. $\mathbf{u}(x, 0, z, t) = \mathbf{a}_{\mathrm{w}}(x, z, t)$, no pressure condition.
2. Inlet: velocity. $\mathbf{u}(\overline{x}, y, z, t) = \mathbf{a}_{\mathrm{i}}(y, z, t)$, no pressure condition.
3. Lateral sides: periodicity. $\mathbf{u}(x, y, -S, t) = \mathbf{u}(x, y, S, t)$, $p(x, y, -S, t) = p(x, y, S, t)$.
4. Outlet: Flow alignment, $\hat{\boldsymbol{\tau}}_\ell \cdot \mathbf{u}(\overline{x} + L, y, z, t) = 0$, $\hat{\boldsymbol{\tau}}_1 = \hat{\mathbf{y}}$, $\hat{\boldsymbol{\tau}}_2 = \hat{\mathbf{z}}$. + Derivative condition for the normal component $\partial_x u(\overline{x} + L, y, z, t) = 0$ + pressure, $p(\overline{x} + L, y, z, t) = c_{\mathrm{o}}(y, z, t)$.
5. At infinity, asymptotic conditions on u_x and u_z and pressure:

$$\lim_{y \to \infty} \hat{\boldsymbol{\tau}}_\ell \cdot \mathbf{u}(x, y, z, t) = \hat{\boldsymbol{\tau}}_\ell \cdot \mathbf{a}_\infty(x, z, t),$$

$$\lim_{y \to \infty} p(x, y, z, t) = c_\infty(x, z, t),$$

with $\hat{\boldsymbol{\tau}}_1 = \hat{\mathbf{x}}$ and $\hat{\boldsymbol{\tau}}_2 = \hat{\mathbf{z}}$.

The spectral expansion

Expansion depends on boundary conditions.
After Fourier expansion in the z direction

$$u_x^m(\xi,\eta) = \sum_{i=0}^{I}\sum_{j=0}^{J} L_i^{\mathrm{DN}}(\xi)\, v_{x;i,j}^m\, \mathcal{B}_j(\eta) \quad \underbrace{+\, a_{x,\infty}^m(x(\xi),y(\eta))}$$

$$u_y^m(\xi,\eta) = \sum_{i=0}^{I}\sum_{j=0}^{J} L_i^{*}(\xi)\, v_{y\star;i,j}^m\, \mathcal{B}_j^{\star}(\eta) \quad \underbrace{+\, d^m(x(\xi),y(\eta))\, y},$$

$$u_z^m(\xi,\eta) = \sum_{i=0}^{I}\sum_{j=0}^{J} L_i^{*}(\xi)\, v_{z;i,j}^m\, \mathcal{B}_j(\eta) \quad \underbrace{+\, a_{z,\infty}^m(x(\xi),y(\eta))},$$

$$p^m(\xi,\eta) = \sum_{i_h=0}^{\hat{I}}\sum_{\hat{\jmath}=0}^{\hat{J}} L_{i_h}^{\mathrm{ND}}(\xi)\, q_{i_h,\hat{\jmath}}^m\, \mathcal{B}_{\hat{\jmath}}(\eta) \quad \underbrace{+\, c_{\infty}^m(x(\xi),y(\eta))},$$

asymptotic terms.

The discrete problem

After discretization and lifting, the discrete linear systems become:

$$
\begin{aligned}
u_x: &\quad \boldsymbol{\mathcal{V}}^m M_\infty + r_y^2 \mathcal{M} \boldsymbol{\mathcal{V}}^m + \chi_\gamma^{|m|} \mathcal{M} \boldsymbol{\mathcal{V}}^m M_\infty = \boldsymbol{\mathcal{G}}^m, \\
u_y: &\quad \mathbf{V}^m M_\infty^{\star\, T} + r_y^2 M \mathbf{V}^m D_\infty^{\star\, T} + \kappa_\gamma^{|m|} M \mathbf{V}^m M_\infty^{\star\, T} = \mathbf{G}^m, \\
u_z: &\quad \mathbf{V}^m M_\infty + r_y^2 M \mathbf{V}^m + \chi_\gamma^{|m|} M \mathbf{V}^m M_\infty = \mathbf{G}^m, \\
p: &\quad \mathbf{Q}^m M_\infty + r_y^2 M \mathbf{Q}^m D_\infty + \kappa_\gamma^{|m|} M \mathbf{Q}^m M_\infty = \mathbf{G}^m,
\end{aligned}
$$

Some interesting properties

All the matrices on the left-hand side are sparse!!

1. $\mathcal{M}$ and M are pentadiagonal
2. M_∞ is tridiagonal
3. $M_\infty^\star$ and $D_\infty^\star$ are quasi-tridiagonal
4. $M_\infty^\star$ can be factored in closed form

The discrete operators

Not only are the mass and stiffness operators sparse, but the gradient and divergence operators also are.
Here is an outline of the operator patterns.

$\mathcal{M}$ mass matrix

$$
\begin{array}{c}
 \\
1 \\
2 \\
3 \\
4 \\
\vdots \\
I-2 \\
I-1 \\
I
\end{array}
\begin{array}{c}
\begin{array}{ccccccccc} 1 & 2 & 3 & 4 & \cdots & I-2 & I-1 & I \end{array} \\
\begin{pmatrix}
c_1 & b_1 & a_1 & & & & & \\
b_1 & c_2 & 0 & a_2 & & & & \\
a_1 & 0 & c_3 & 0 & \ddots & & & \\
 & a_2 & 0 & c_4 & 0 & \ddots & & \\
 & & \ddots & 0 & \ddots & 0 & a_{I-3} & \\
 & & & \ddots & 0 & c_{I-2} & 0 & a_{I-2} \\
 & & & & a_{I-3} & 0 & c_{I-1} & 0 \\
 & & & & & a_{I-2} & 0 & c_I
\end{pmatrix}
\end{array}
$$

The discrete operators

Not only are the mass and stiffness operators sparse, but the gradient and divergence operators also are.
Here is an outline of the operator patterns.

M mass matrix

$$
\begin{array}{c} \\ 2 \\ 3 \\ 4 \\ \vdots \\ I-2 \\ I-1 \\ I \end{array}
\begin{array}{c}
\begin{array}{ccccccc} 2 & 3 & 4 & \cdots & I-2 & I-1 & I \end{array} \\
\begin{pmatrix}
c_2 & 0 & a_2 & & & & \\
0 & c_3 & 0 & \ddots & & & \\
a_2 & 0 & c_4 & 0 & \ddots & & \\
 & \ddots & 0 & \ddots & 0 & a_{I-3} & \\
 & & \ddots & 0 & c_{I-2} & 0 & a_{I-2} \\
 & & & a_{I-3} & 0 & c_{I-1} & 0 \\
 & & & & a_{I-2} & 0 & c_I
\end{pmatrix}
\end{array}
$$

The discrete operators

Not only are the mass and stiffness operators sparse, but the gradient and divergence operators also are.
Here is an outline of the operator patterns.

M_∞ mass matrix

$$M_\infty = \begin{array}{c} \\ 1 \\ 2 \\ 3 \\ \vdots \\ J-1 \\ J \end{array} \begin{array}{c} \begin{array}{cccccc} 1 & 2 & 3 & \cdots & J-1 & J \end{array} \\ \begin{pmatrix} 2 & -1 & & & & \\ -1 & 2 & -1 & & & \\ & -1 & \ddots & \ddots & & \\ & & \ddots & \ddots & \ddots & \\ & & & \ddots & \ddots & -1 \\ & & & & -1 & 2 \end{pmatrix} \end{array}$$

The discrete operators

Not only are the mass and stiffness operators sparse, but the gradient and divergence operators also are.
Here is an outline of the operator patterns.

$M^\star_\infty$ mass matrix

$$M^\star_\infty = \begin{array}{c} \\ 1 \\ 2 \\ 3 \\ \vdots \\ J-1 \\ J \end{array} \begin{array}{c} \begin{array}{ccccccc} 1 & 2 & 3 & \cdots & J-1 & & J \end{array} \\ \begin{pmatrix} 2 & -1 & & & & & 3 \\ -1 & 2 & -1 & & & & -4 \\ & -1 & \ddots & \ddots & & & +4 \\ & & \ddots & \ddots & \ddots & & \vdots \\ & & & -1 & 2 & (-1)^{J-2}4 \\ & & & & -1 & (-1)^{J-1}4 \end{pmatrix} \end{array}$$

The discrete operators

Not only are the mass and stiffness operators sparse, but the gradient and divergence operators also are.
Here is an outline of the operator patterns.

$D^\star_\infty$ mass matrix

$$D^\star_\infty = \begin{array}{c} \\ 1 \\ 2 \\ 3 \\ \vdots \\ J-1 \\ J \end{array} \begin{array}{c} \begin{array}{ccccccc} 1 & 2 & 3 & \cdots & J-1 & J \end{array} \\ \begin{pmatrix} 2 & 1 & & & & 1 \\ 1 & 2 & 1 & & & \\ & 1 & \ddots & \ddots & & \\ & & \ddots & \ddots & 1 & \\ & & & 1 & 2 & 0 \\ & & & & 1 & 0 \end{pmatrix} \end{array}$$

Convergence results

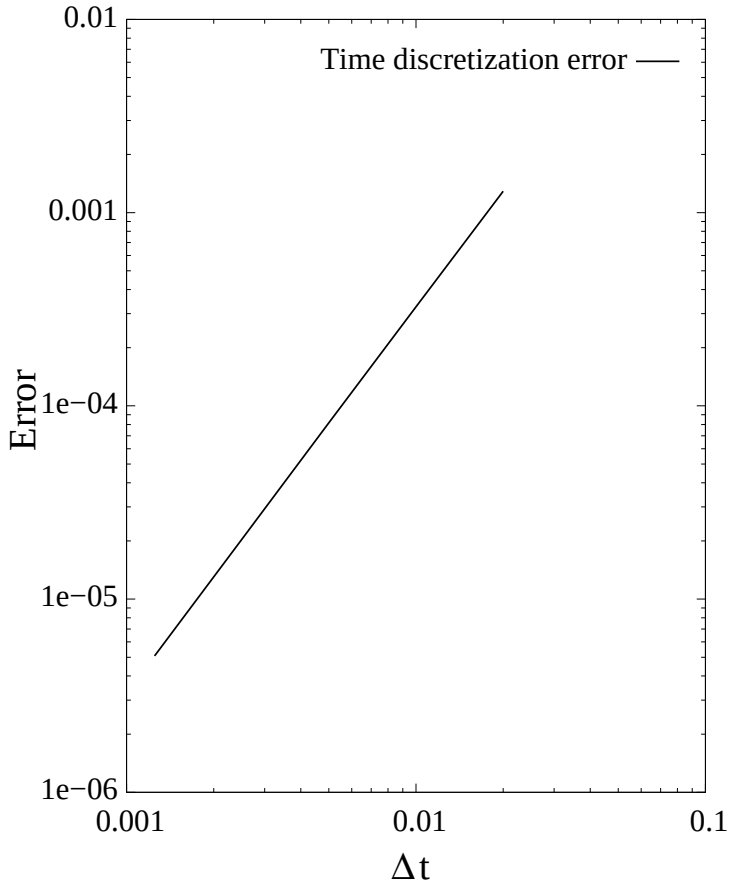

Second order accuracy in time

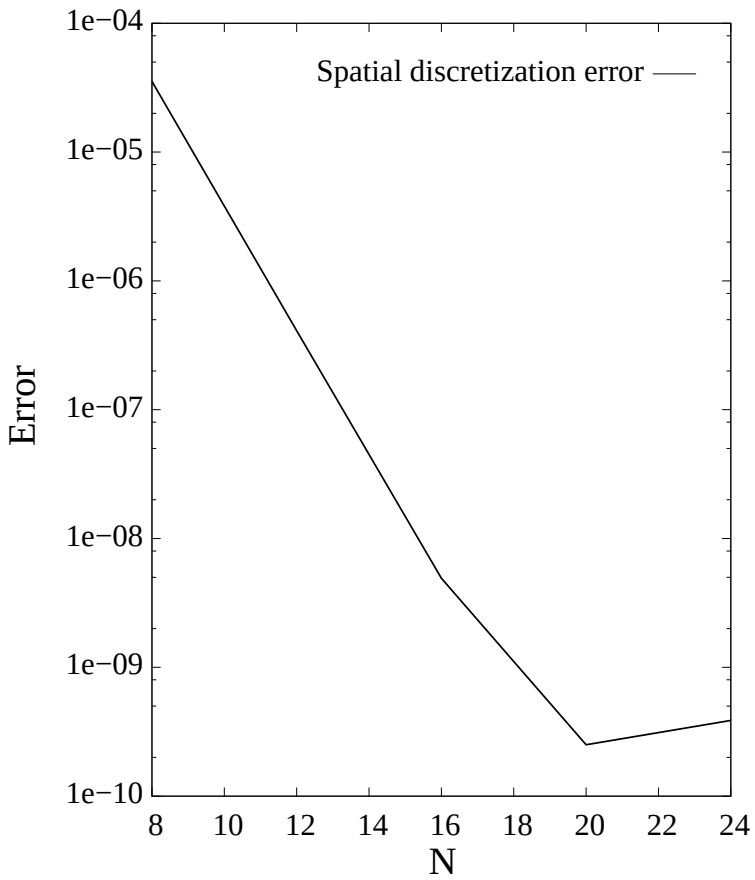

Spectral accuracy in space

Blasius boundary layer

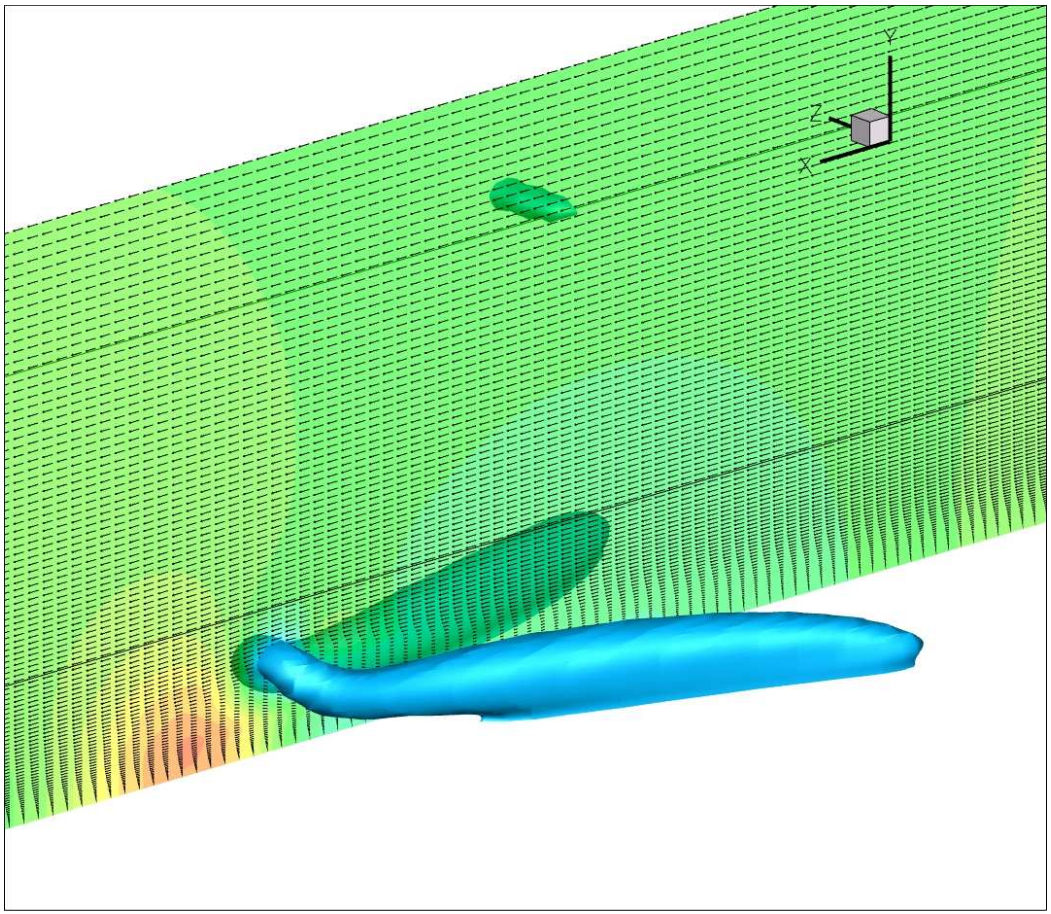

Evolution of a hairpin vortex ($\mathrm{Re}_{\delta^*} = 50000$).
Discretization: dealiased $768 \times 128 \times 128$

Blasius boundary layer

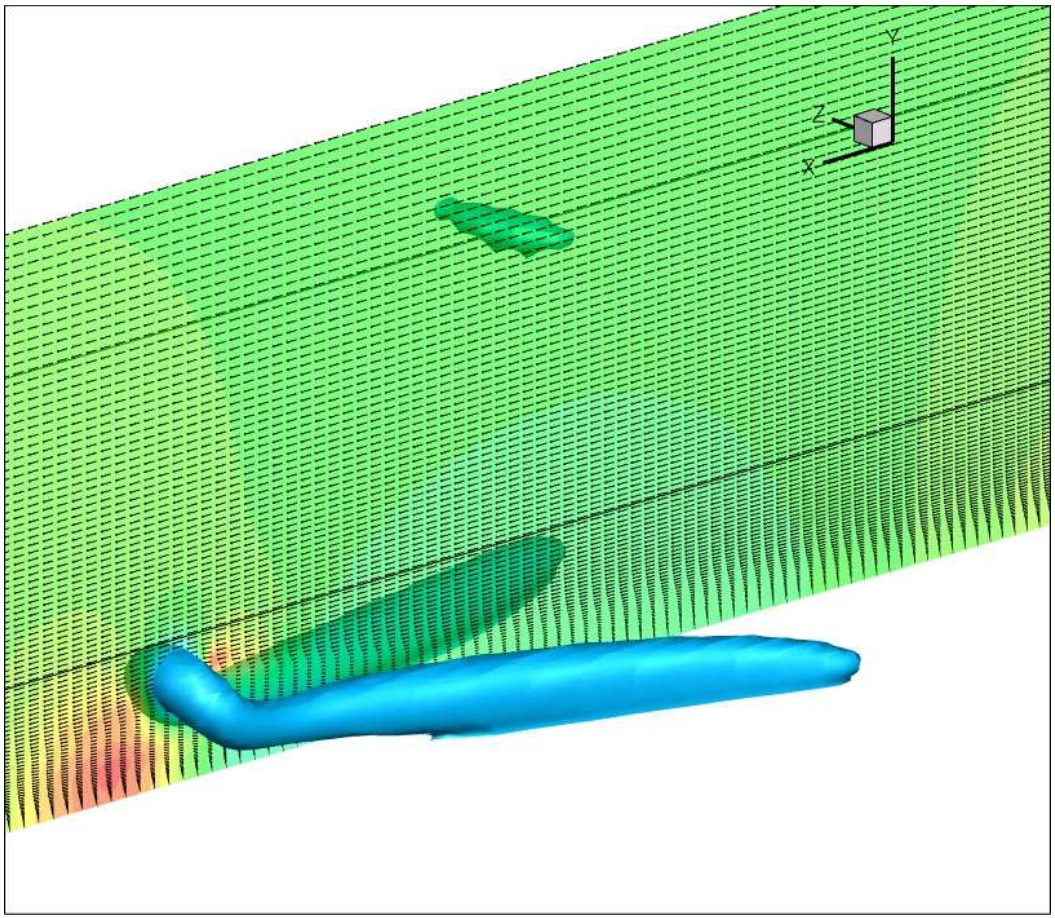

Evolution of a hairpin vortex ($\mathrm{Re}_{\delta^*} = 50000$).
Discretization: dealiased $768 \times 128 \times 128$

Blasius boundary layer

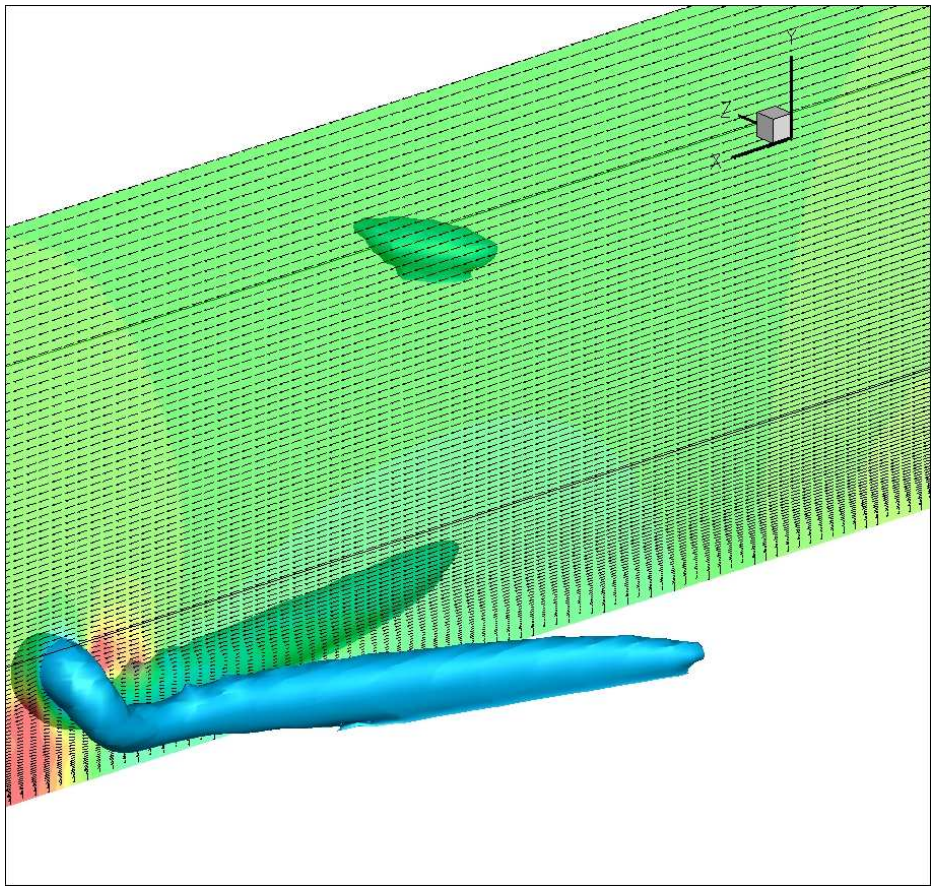

Evolution of a hairpin vortex ($\mathrm{Re}_{\delta^*} = 50000$).
Discretization: dealiased $768 \times 128 \times 128$

Outline

A quasi-optimal fractional-step method for the Navier–Stokes equations in non-periodic boxes

Motivation

Efficiently solving Navier–Stokes equations in non-periodic boxes could be crucial to investigate:

1. Flows in ducts with rectangular cross section;
2. Spatially developing flows;
3. Flows in simple enclosures;
4. End effects in natural convection;
5. Domain decomposition extension to more complicate geometries;
6. ...

Preliminaries

Singular perturbation of the Stokes problem:

$$\begin{cases} \frac{\partial \mathbf{u}_\epsilon}{\partial t} - \nu \nabla^2 \mathbf{u}_\epsilon + \boldsymbol{\nabla} p_\epsilon = \mathbf{f} \quad \text{in } \Omega \times [0, T], \\ \Delta t A p_\epsilon + \boldsymbol{\nabla} \cdot \mathbf{u}_\epsilon = 0 \quad \text{in } \Omega \times [0, T] \\ + \text{i.c. and b.c.} \end{cases}$$

$A : D(A) \subset L^2_{\int=0}(\Omega) \to L^2_{\int=0}(\Omega)$: bounded and closed operator, such that $a(p, q) \triangleq \int_\Omega qAp$ is symmetric and $\|\boldsymbol{\nabla} q\|^2_{L^2} \leq a(q, q)$, $\forall q \in D(A)$.

Theorem (Guermond and Minev, 2011)

If the solution $\mathbf{u}$ to the Stokes problem is smooth enough wrt time and space and if previous conditions hold, then the solution $\mathbf{u}_\epsilon$ to the perturbed system satisfies the estimate (as the singular perturbation understood by Chorin–Temam projection method).

$$\|\mathbf{u} - \mathbf{u}_\epsilon\|_{L^2((0,T);H^1(\Omega))} \leq c \Delta t^{1/2}$$

Direction splitting fractional step method (Guermond and Minev, 2010)

First step: velocity update

$$\frac{\mathbf{w}^{k+1}-\mathbf{u}^{k}}{\Delta t}-\frac{\nu}{2}\partial_{xx}(\mathbf{w}^{k+1}-\mathbf{u}^{k})=\mathbf{f}^{k+1/2}+\nu\nabla^{2}\mathbf{u}^{k}$$

$$-(\mathbf{u}_{\star}^{k+1/2}\cdot\boldsymbol{\nabla})\mathbf{u}_{\star}^{k+1/2}-\boldsymbol{\nabla}p_{\star}^{k+1/2}+\text{b.c.}$$

$$\frac{\mathbf{v}^{k+1}-\mathbf{w}^{k+1}}{\Delta t}-\frac{\nu}{2}\partial_{yy}(\mathbf{v}^{k+1}-\mathbf{u}^{k})=0+\text{b.c.}$$

$$\frac{\mathbf{u}^{k+1}-\mathbf{v}^{k+1}}{\Delta t}-\frac{\nu}{2}\partial_{zz}(\mathbf{u}^{k+1}-\mathbf{u}^{k})=0+\text{b.c.}.$$

Direction splitting fractional step method (Guermond and Minev, 2010)

Second step: pressure update

$$\begin{cases} (1-\partial_{xx})\psi = -\dfrac{1}{\Delta t}\boldsymbol{\nabla}\cdot\mathbf{u}^{k+1}, & \partial_x\psi|_{\xi=\pm1} = 0 \\ (1-\partial_{yy})\varphi = \psi, & \partial_y\varphi|_{\eta=\pm1} = 0 \\ (1-\partial_{zz})\phi^{k+1/2} = \varphi, & \partial_z\phi^{k+1/2}|_{\zeta=\pm1} = 0 \end{cases}$$

$$p^{k+1/2} = p^{k-1/2} + \phi^{k+1/2} - \chi\frac{\nu}{2}\boldsymbol{\nabla}\cdot(\mathbf{u}^{k+1}+\mathbf{u}^{k}).$$

Guermond and Minev tried second order finite differences: fast, not very accurate.
Shen et al. tried Legendre polynomials: accurate, not very fast.

Choosing the appropriate basis

Problem: which basis

- Choosing the appropriate basis is **key** to obtain an efficient algorithm. For instance: Legendre polynomials (Shen et al., 2011) lead to $O(N^4)$-operation algorithms.
- Basis requirements:
  1. each step at least quasi-optimal ($\leq cN^3 \log N$ flop);
  2. satisfy LBB condition;
  3. well conditioned;
  4. easy fulfillment of boundary conditions;
  5. efficient de-aliasing.

Choosing the appropriate basis

The idea

1. Use Chebyshev polynomials $\rightarrow$ FFT;
2. Use Galerkin pseudospectral (not collocation) $\rightarrow$ LBB and de-aliasing;
3. Use Shen's basis (Shen, 1995) $\rightarrow$ well conditioned, boundary conditions, sparse operators;

The basis

Same basis for Dirichlet, Neumann and mixed problems:

$$\hat{T}_i(\xi) = \begin{cases} 1, & i = 0, \\ \xi, & i = 1, \\ T_{i-2}(\xi) - T_i(\xi), & i \geq 2. \end{cases}$$

Elliptic equation solution

After Galerkin discretization a cascade of N^2 1D linear system like $(\alpha S + \gamma M)V = G$ must be solved;

- The stiffness matrix S is upper triangular with a special structure; mass matrix M is pentadiagonal, symmetric, with two zero diagonals.
- The matrices are factored once and for all in preprocessing;
- Back substitution takes just $\approx 5N$ flop (versus $3N$ for a tridiagonal system);
- Neumann b.c. are converted to Dirichlet b.c. ($+4N \div 7N$ flop)

Gradient and divergence operators

Gradient and divergence are sparse.
The computation is performed in the coefficient space (each matrix multiplication costs as a tridiagonal matrix multiplication):

$$-\frac{\hat{\mathbf{x}}}{L} D_r \overset{M_r^T}{p_\star^{k+1/2}} M_r^T - \frac{\hat{\mathbf{y}}}{H} M_r \overset{M_r^T}{p_\star^{k+1/2}} D_r^T - \frac{\hat{\mathbf{z}}}{B} M_r \overset{D_r^T}{p_\star^{k+1/2}} M_r^T$$

M_r mass operator. D_r first derivative operator:

$$\begin{pmatrix} 0 & \pi & 0 & -2\pi & 0 & -2\pi \\ 0 & 0 & -2\pi & 0 & -2\pi & 0 \\ & \pi & 0 & \pi & & \\ & & -2\pi & 0 & 2\pi & \\ & & & -3\pi & 0 & 3\pi \\ & & & & -4\pi & 0 \end{pmatrix}.$$

Results: convergence

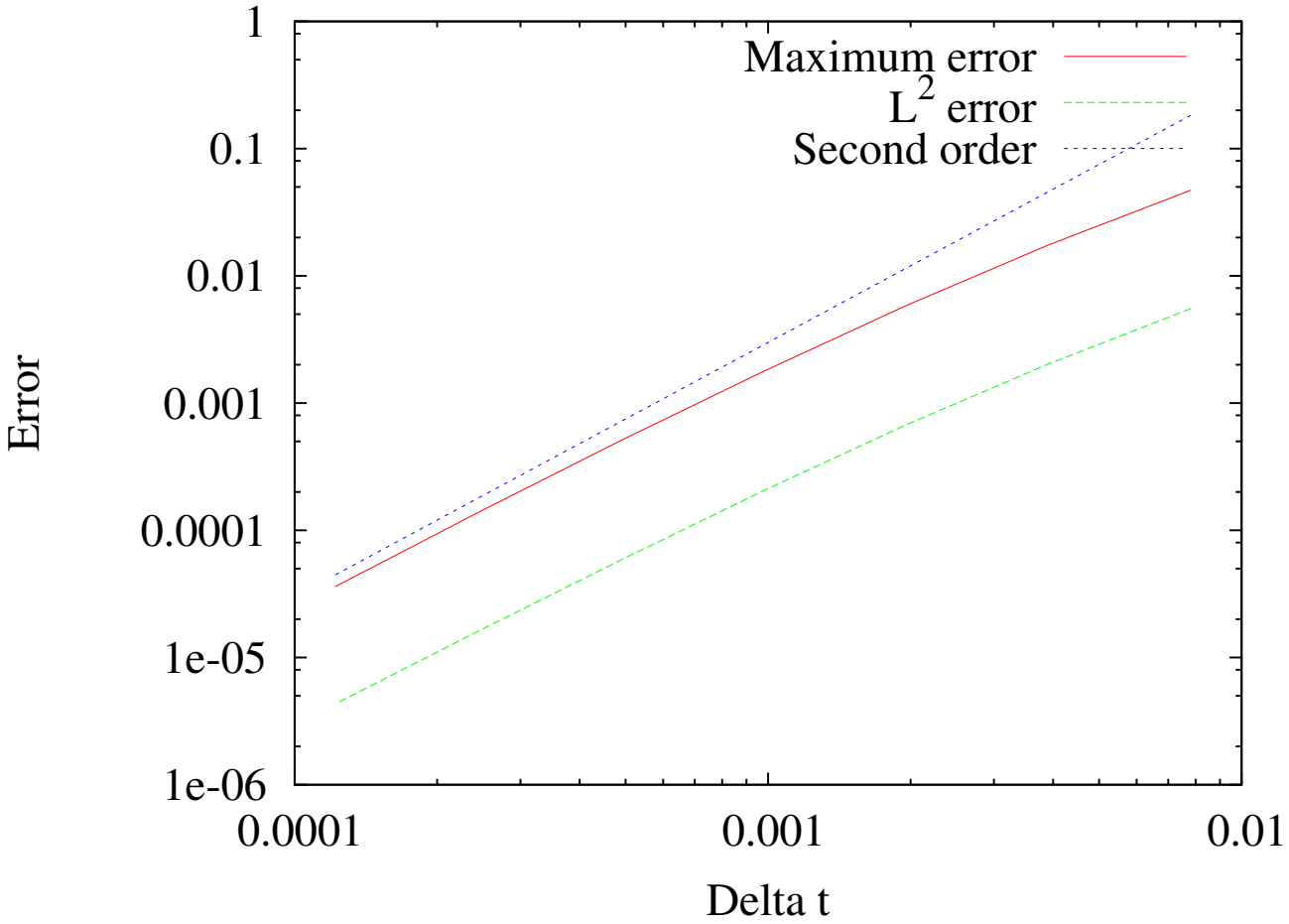

Second order accuracy (for small time steps).

Results: oscillating cavity

$\mathrm{Re} = 1250$

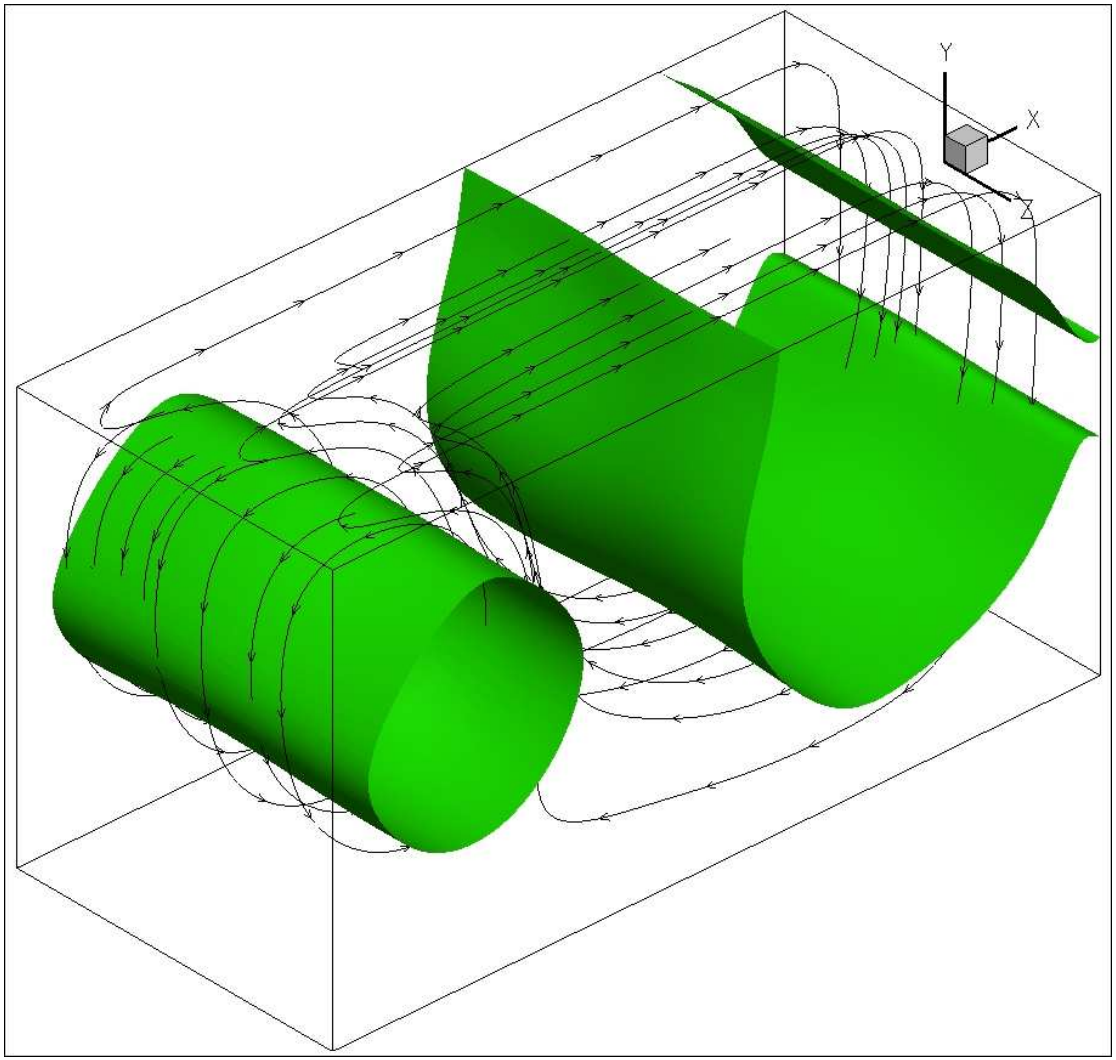

Results: oscillating cavity

$\mathrm{Re} = 1250$

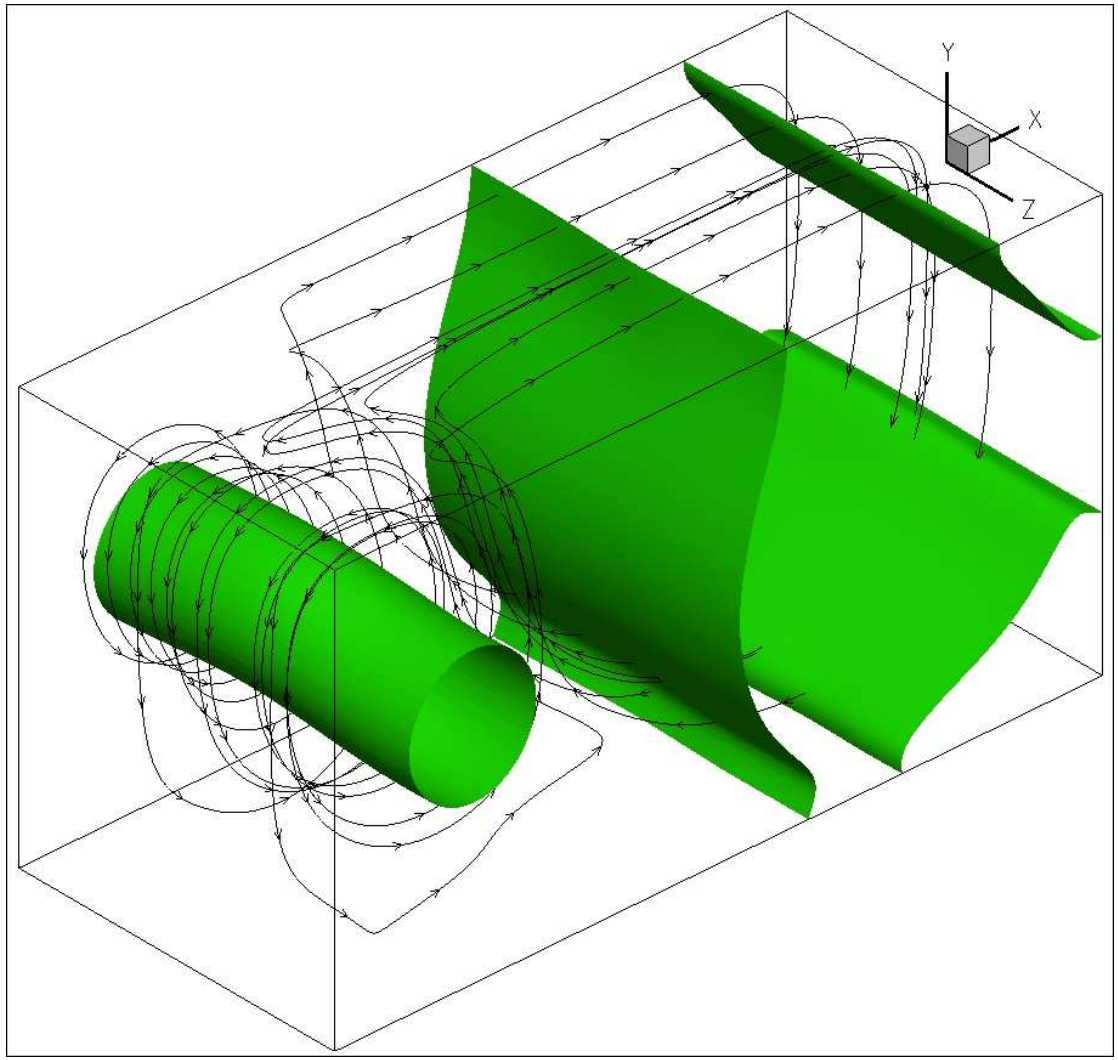

Results: oscillating cavity

$\mathrm{Re} = 1250$

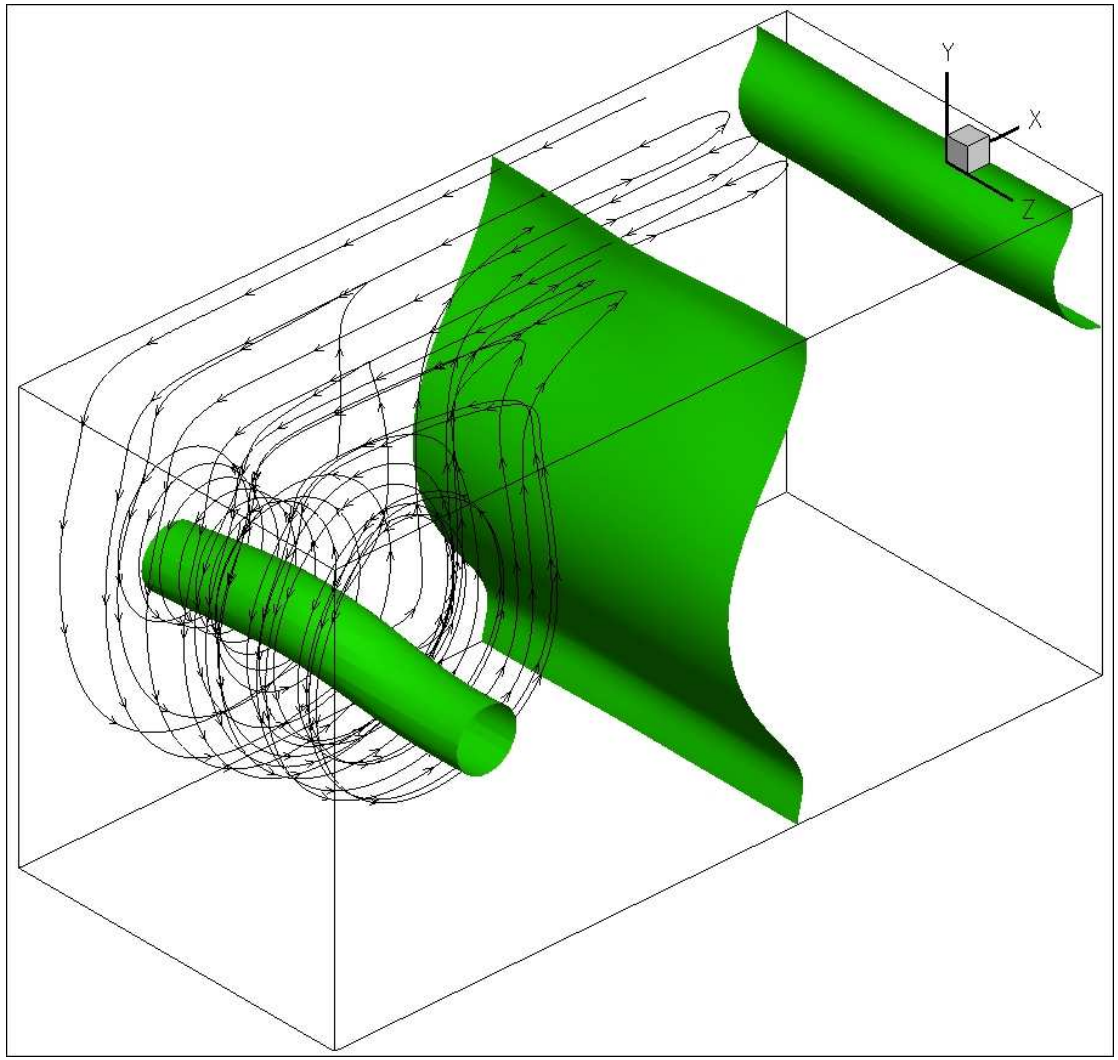

Outline

Summary

New spectral elliptic solvers fluid mechanics equation in non-Cartesian coordinates, open and closed regions have been developed that:

1. are numerically stable
2. are spectrally accurate
3. are efficient

Thank you for your kind attention.